# Numerical analysis of flow characteristics of a fluid flowing through an orifice in a marine piping system

A thesis submitted in partial fulfilment of the requirements for the award of Master of Technology in Marine Technology


**By**

**AVIJIT MAJI**

(Reg. No.: 2201215001)


Under the guidance of

**Dr. SUJAY SAHA**

(Faculty, IMU Kolkata Campus)


**Department of Marine Engineering**

**Indian Maritime University Kolkata Campus**

**Kolkata 700088**


**July 2024**

# INDIAN MARITIME UNIVERSITY KOLKATA CAMPUS

DEPARTMENT OF MARINE ENGINEERING

# CERTIFICATE

This research is to certify that the thesis entitled **"Numerical analysis on flow characteristics of a fluid, flowing through an orifice, in a marine piping system"** is submitted by **"Avijit Maji"** (2201215001) of the Department of Marine Engineering, Indian Maritime University (Kolkata campus), in a partial full film of the requirement for the award of the degree of **Master of Technology** in Marine Technology, is record of bonafide research work carried out under my supervision and guidance.

The content of the dissertation does not form a basis for the award of other degrees to his/her, to the best of my knowledge. The dissertation, in my opinion, is worthy of consideration for the award of the degree **Master of Technology** in Marine Technology following the regulations of the institute.

| | | |
|---|---|---|
| **Dr. Sujay Saha**<br>Supervisor<br>Indian Maritime University<br>Kolkata Campus,<br>Kolkata, West Bengal 700088<br>India | **Dr. Amarish Kumar Shukla**<br>Course Coordinator<br>Indian Maritime University<br>Kolkata Campus,<br>Kolkata, West Bengal 700088<br>India | **External Examiner** |

# EVALUATION SHEET

| | |
|---|---|
| Name of candidate: | Avijit Maji |
| Title of the project: | NUMERICAL ANALYSIS OF FLOW CHARACTERISTICS OF A FLUID, FLOWING THROUGH AN ORIFICE, IN A MARINE PIPING SYSTEM. |
| Specialization: | Marine Technology |
| Date of Examination: | |

The board approved this dissertation for the exam.

External Examiner:

Internal Examiner:

# COPYRIGHT AND CONSENT FORM

To ensure uniformity of treatment among all contributors, other forms may not be substituted for this form, nor may any wording of the form be changed. This form is intended for original material submitted to the Indian Maritime University, Kolkata Campus (IMU-KC), Kolkata and must accompany any such material to be published by the (IMU-KC). Please read the form carefully and keep a copy for your files.

TITLE OF THESIS: Numerical analysis on flow characteristics of a fluid, flowing through an orifice, in a marine piping system.

AUTHOR'S NAME and ADDRESS: Avijit Maji , Bora, Bonra, Purulia, West Bengal, Pin-723121

# COPY RIGHT TRANSFER

- The undersigned hereby assigns to Indian Maritime University, Kolkata Campus (IMUKC), Kolkata, all rights under copyright that may exist in and to: (a) the above work, including any revised or expanded derivative works submitted to the (IMU-KC), by the undersigned based on the work and (b) any associated written or multimedia components or other enhancements accompanying the work.

# CONSENT AND RELEASE

- In the event of undersigned makes a presentation based upon the work at a conference hosted or sponsored in whole or in part by the (IMU-KC), the undersigned, in consideration for his/her participation in the conference, hereby grants the (IMU-KC), the unlimited, worldwide, irrevocable permission to use, distribute, publish, license, exhibit, record, digitize, broadcast, reproduce and archive, in any format or medium, Whether now known or hereafter developed : (a) his/her presentation and comments at the conference: (b) any written materials or multimedia files used in connection with his/her presentation and : (c) any recorded interview him/her (collectively, the “Presentation” ). The permission granted includes the transcription and reproduction of the Presentation for inclusion in products sold or distributed by (IMU-KC) and a live or recorded broadcast of the Presentation during or after the conference. In connection with the permission granted in

Section 2, the undersigned hereby grants (IMU-KC) the unlimited, worldwide, irrevocable right to use his/her name, picture, likeness, voice, and biographical information as part of the advertisement, distribution, and sale of products incorporating the Work or Presentation, and releases (IMU-KC) from any claim based on the right of privacy or publicity.

- The undersigned individual, in relation to the permission granted in Section 2, gives (IMU-KC), the unrestricted, global, and irreversible permission to utilize their name, image, resemblance, voice, and biographical for promotional purposes, including the advertisement, distribution, and sale of products that feature the Work or Presentation. Additionally, the undersigned releases (IMU-KC) from any potential claims related to privacy or publicity rights.
- The person signing this document affirms that the Work and Presentation (referred to as the "Materials") are authentic and that they are the creator of the Materials. If the Materials include any test passages figures, data or other content from someone else's work, the undersigned obtained all required permissions.

# GENERAL TERMS

- The undersigned represents that he/she has the power and authority to make and execute this assignment.
- The undersigned agrees to indemnify and hold harmless the (IMU-KC) from any damage or expense that may arise in the event of a breach of any of the warranties set forth above.
- In the event the above work is not accepted and published by the (IMU-KC) or is withdrawn by the author(s) before acceptance by the (IMU-KC), the foregoing copyright transfer shall become null and void and all materials embodying the work submitted to the (IMU-KC) will be destroyed.
- For jointly authored works, all joint authors should sign, or one of the authors should sign as an authorized agent for the others.

Avijit Maji
(Reg. no.: 2201215001)
Master of Technology
Dept. of Marine Engineering
Indian Maritime University
Kolkata

# Table of Contents

# ACKNOWLEDGEMENTS

It gives me great pleasure to acknowledge the assistance and direction I received from many people to prepare this report. This report could not have been prepared in its current form without their invaluable help, collaboration, and direction. First and foremost, we would like to express our profound gratitude to the Indian Maritime University's administration in Kolkata and our esteemed Director, Shir. Dr. Rangachari PJ, for their unwavering support and encouragement during the preparation of this report and for providing the required laboratory and library resources.

I express my gratitude to Senior Professor Dr. Sujay Saha of the Department of Marine Engineering at Imu Kolkata for his insightful advice in supervising my research for this project and for guiding this report. I sincerely thank Dr. Amarish Kumar Shukla, Course Coordinator, Department of Marine Engineering, IMU Kolkata, for his inspiration and assistance in finishing the project.

Additionally, IMU Kolkata has provided all lab facilities with computers loaded with the necessary software to complete the work efficiently and facilitate the project design and analysis, for which I sincerely thank them.

# DECLARATION

I certify that

1. The work contained in the species is original and has been done by me under the guidance of my superior.
2. The work has not been submitted to any other institute for any degree or diploma.
3. I have followed the guidelines provided by the institute in preparing this dissertation.
4. I have confirmed the norms and guidelines given in the ethical code of conduct of the institute.
5. Whenever I have used materials (data, theoretical analysis, figure, and text) from other sources, I have given due credit to them by citing them in the text of the thesis and giving the details in reference.

Avijit Maji
(Reg. no.: 2201215001)
Master of Technology
Dept. of Marine Engineering
Indian Maritime University
Kolkata

# LIST OF FIGURES

# LIST OF TABLE

# LIST OF EQUATION

# ABSTRACT

Over the last few decades expensive research work has been performed by many researchers on the monitoring of rate of fluid flow through various pipes. Moreover, in the marine industry, it's important to conduct a detailed analysis of the uncertainties associated with flow measurement. It has been also seen that the coefficients, which are used for orifices are based on empirical data. Therefore, accurately predicting the impact of complex geometry and flow separation from the orifice in the flow have become crucial challenges for many researchers. From the review of the literature, it has been noted that a systematic detailed investigation of the flow through the orifice has not been done so far. Thus, in the present study a systematic details numerical investigation has been conducted for incompressible turbulent flow of water through a square edge orifice plate with considering various Reynolds numbers ranging from $15^3$ to $27^3$ and Bita ratios from $0.3432$ to $0.6289$. The standard design of ISO 5167-2 has been used in the present investigation. In this work, the simulations have been performed by using the ANSYS Fluent. The standard k-ε model has been selected for the turbulence flow analysis. The streamline contour, velocity contour, pressure contour, centreline axial velocity, wall pressure, radial profile of turbulent kinetic energy, and turbulent dissipation rate are presented in the results and discussion section in a systematic manner. From the analysis, it has been noted that the pressure drops from the orifice plate up to the vena contracta increase with increasing the Reynolds numbers and the beta ratio. It has also been observed that the pressure affects the jet-like flow in the core region, the recirculation zone, the reattachment, and the shear regions on the downstream side of the orifice. The location of vena contracta is also be estimated from present CFD simulations. Thus, this analysis improves the accuracy of coefficients. Consequently, error may be minimized in view of monitoring the rate of fluid flow in marine systems.

# CHAPTER 1

## 1.1 Introduction

The orifice plate commonly used for measuring flow in fluid distribution systems is an orifice plate that generates a pressure drop across the plate and is placed into a pipe. The flow rate of the pipe helps to calculate the pressure drop. The fluid's pressure slightly rises upstream as it passes through the orifice and then the pressure drops as it converges to fit through the opening. The flow reaches the vena contracta, a region of maximum convergence when the pressure reduces and velocity peaks. Bernoulli's equation and coefficients, derived from a great deal of study, can be used to calculate flow rates by measuring the pressure differential across the orifice. When a fluid is single-phase, well-mixed, continuous, and satisfies certain flow requirements, orifice plates are frequently utilized. To achieve precise flow rate determination, they are installed and designed according to the needs of the sector. Depending on the requirement, we used square edge, quadrant, conic edge, integral, eccentric, and segmental orifice plates [1-2].

*Figure 1: Orifice fitted in a pipe.*

In the ship pipe systems orifice plates are also widely used for flow monitoring and control due to their simplicity, dependability, and cost-effectiveness. However, turbulent flow conditions — which are typical in maritime systems—can significantly affect the accuracy of flow measurement using orifice plates. Turbulent flow generates uncertainty in pressure drop and flow rate measurements, which may contribute to system operation and maintenance inaccuracies. As a result, understanding the flow characteristics of orifice plates in turbulent flow conditions is critical for accurate flow measurement and optimal system performance.

Numerical and CFD models are becoming more essential methods for marine engineering research, providing an affordable and effective means for evaluating complicated flow processes. This study uses these methods to investigate how orifice plates in ship pipe systems affect the flow of fluids when the flow is turbulent. It focuses on the pressure drop, measuring flow rate, and energy loss that are connected to these devices.

## 1.2 Background of this Research

The investigation of fluid flow is a crucial aspect of several technical applications, especially in handling different fluids. Around 5000 B.C., the people of Mesopotamia invented the concept of water distribution control through the measurement of flows across obstructions in channels. In 1450, Battista Alberti produced the first mechanical anemometer to measure wind speed, which later led to the development of various types of flow meters. Thus, precise flow measurement is still required for process control in modern processing plants [3]. Ships must optimize energy efficiency and enhance safety as they transport over 80% of all global trade goods by using proper flow measurements. Orifice plates are widely used in this context to measure and control flow rates in onboard systems such as fuel lubrication, water distribution, and steam propulsion systems [4, 7]. Orifice plate technology employed on board oil tankers in 1995 that can make water, illustrating their adaptability and significance in marine operations [5,6].

Specific industrial needs and fluid characteristics dictate the use of different types of orifice plates, including concentric, eccentric, segmental, and quadrant orifice plates. The concentric orifice plates are commonly used for clean liquids, gases, and steam flows, and eccentric and segmental ones for fluids with particles or slurries. Quadrant orifice plates are designed to measure viscous fluid under certain conditions [8, 9,]. Marine engineering relies on a comprehension of fluid dynamics in general and the distinction between laminar and turbulent flows specifically. Whereas laminar flow is smooth and orderly and hence predictable when needed in some applications, turbulent flow is chaotic, thus it promotes mixing as well as heat transfer, which is useful in various industries [10,14]. Reynolds numbers, a dimensionless parameter that is essential for optimizing fluid systems on ships [11, 12,13], signal the change from one type of flow to another.

The Reynolds number, a dimensionless parameter based on velocity, pipe size, and fluid viscosity, determines the transition between laminar and turbulent flow. A low Reynolds number indicates laminar flow, while a high Reynolds number indicates turbulent flow. Understanding these flow types is crucial in fluid-dynamics problems as they affect heat and mass transfer in fluid systems. Because of turbulence cavitation forms in the orifice plate and the pipe boundary. Cavitation, a phenomenon in fluid mechanics, refers to the formation of small vapor-filled cavities or bubbles

when the static pressure of the liquid reduces to below the liquid's vapor pressure. Turbulent effects on fluid flow systems, such as those involving an orifice plate, are a significant concern in marine engineering. Turbulent flow through an orifice plate can increase pressure and stress, affecting its performance and overall flow dynamics. The Reynolds number, a dimensionless parameter used to predict the transition from laminar to turbulent flow, is directly related to flow velocity and pressure and stress acting on the orifice plate. The thickness-to-diameter ratio of the orifice plate can also influence turbulent flow behaviour, impacting flow characteristics and pressure distribution around the plate. Turbulent effects on the orifice plate can lead to increased pressure drop across the orifice plate, resulting in reduced accuracy of flow measurement and increased erosion of the orifice plate and surrounding piping, reducing the lifespan of the equipment. Mitigation strategies for turbulent effects on the orifice plate include using a larger orifice plate diameter and employing turbulence-reducing devices like vortex generators [15].

We conduct the computational fluid dynamics (CFD) analysis of an orifice plate using ANSYS Fluent 2024, turbulence-induced cavitation, and its effects on the orifice plate. The software allows for the simulation of complex fluid flow phenomena, including turbulence's impact on pressure and stress distribution across the orifice plate. The turbulent effects are characterized by the Reynolds number, a dimensionless parameter. The analysis also considers the thickness-to-diameter ratio of the orifice plate and its influence on turbulent flow behavior. We explore turbulence mitigation strategies like using a larger orifice plate diameter and turbulence-reducing devices. The software also considers the flow conditions upstream of the orifice plate, as they can influence the turbulent effects on the plate. This CFD analysis with ANSYS Fluent 2024 is very important for improving the accuracy of flow measurements, the efficiency of systems, and the durability of equipment used in marine engineering and other fluid flow applications.

## 1.3 Literature Review

The use of orifice plates in various industrial applications for flow measurement is both widespread and vital due to their cost-effectiveness, reliability, and simplicity. However, the performance and accuracy of these devices can be significantly affected by various factors, including contamination, geometric variations, and flow conditions. The following research studies delve into these aspects, providing valuable insights into the implications for orifice plate design and application.

N. Abed et al. [16] conducted a test and numerical think about, how turbulent discuss moves through a circular hole to look at the wonder of stream division and reattachment close the hole. They have utilized a circular opening plate for both exploratory strategies (such as hot-wire

anemometry and Pitot tubes) and numerical reenactments (utilizing CFD with ANSYS Familiar). To analyse speed, turbulent dynamic vitality, and Reynolds stresses utilizing the standard k-ε and Reynolds Push Show (RSM). Boundary conditions comprised of a uniform speed profile at the gulf for a Reynolds number of 30,000, weight outlet conditions, and no-slip conditions on the dividers. Approval utilizing test information appeared that RSM is more precise for anisotropic streams, indeed in spite of the fact that it takes longer to compute than the k-ε shows. This investigation offers profitable experiences for optimizing hole plate plans in designing applications, highlighting the noteworthiness of choosing the right turbulence model.

Erdal et al. [17], have conducted a consider of the numerical angles of stream computation through holes. Utilizing computational liquid flow (CFD) apparatuses to pick up unmistakable quality in demonstrating and dissecting prepare frameworks, there is a developing intrigue in recreating metering stations that incorporate stream conditioners (FCs) and hole meters. Be that as it may, this procedure can be completely misused, more data and approval are required in a few ranges. The creators started this consider to investigate different components influencing stream expectations through an hole, counting lattice impacts, arrange courses of action, divider boundary conditions, differencing plans, and turbulence models. The stream calculations for FCs or hole plate in expansion to the approval of the FCs or hole plate are in fact considered to be inspected in a 2d axisymmetric stream model. In rundown, author's work sheds light on the numerical challenges related with opening stream computations, giving important bits of knowledge for engineers and analysts in the field of liquid dynamics.

Ho et al. [18], have conducted a consider seeing at how well cone shaped entrance opening plates work at moo Reynolds numbers. These numbers are frequently utilized to degree stream in gooey liquids, particularly between 25 to 75 and the examination is combining hands-on tests with hypothetical investigation, in arrange to pick up a more profound understanding of how these plates carry on. The essential objective was to upgrade stream expectation exactness through openings utilizing computational liquid flow (CFD) recreations, with Reynolds number (Re) being a pivotal parameter characterizing stream administrations based on liquid speed, thickness, and consistency. We tried twelve cone shaped entrance hole plates with a steady opening breadth (Od) at moo Reynolds numbers (Re) between 40 and 50,000 and orifice-to-pipe distance across proportions ($^2$) between 0.1 and 0.5. The comes about demonstrated that the release coefficient (Cd), relating the genuine stream rate to the hypothetical stream rate, remained moderately consistent inside indicated ranges. Especially, for $\beta = 0.1$, Cd remained consistent inside +1% over the indicated Ruddy run, whereas for $\beta > 0.2$, there was a slight execution decay with a steady

variety of +2%. In general, the comes about appear that cone shaped entrance hole plates can be utilized to degree stream in thick liquids at moo Reynolds numbers. This gives us valuable data around how these liquids carry on, particularly in circumstances where Reynolds numbers are low.

Markatos et all.[19] have conducted a study to look at strategies models for calculating turbulent stream, a complicated marvel that may be seen in numerous distinctive applications. The investigation included an assortment of geometries, counting channels, channels, planes, wakes, boundary layers, and cavities, in expansion to a few stream sorts, such as laminar, transitional, and turbulent streams. In expansion, a assortment of physical marvels were taken into account, counting mass and warm transmission, chemical responses, and combustion. The vitality and species conditions were utilized to direct warm and mass transport, whereas the Navier-Stokes conditions were utilized to administer liquid stream. The transport conditions for turbulent dynamic vitality and scattering rate and the Reynolds push condition for second-moment closure models are two cases of extra conditions that were included to account for turbulence models. The Reynolds number, Prandtl number, Schmidt number, Grashof number, Rayleigh number, Damkohler number, and Zeldovich number were among the flow-control characteristics that were inspected. Numerous other numerical approaches were utilized, counting the ghastly strategy, the limited component strategy, the limited volume strategy, and the limited distinction strategy. Diverse discretization procedures and arrangement strategies were moreover connected. The reenactment comes about were communicated as a run of distinctive numbers and coefficients, and the observational information and expository answers were compared to approve the conclusions. Moreover assessed were the models and methodologies' steadiness and precision. The discoveries give light on how stream parameters, geometry, boundary conditions, and turbulence models influence the rates of warm and mass exchange as well as stream properties. The examination of the different approaches and models moreover included data almost their benefits, disadvantages, applications, limitations, and proposals for assist investigate. It was decided that turbulence calculations are vital for practical reenactments and that more fundamental, prior procedures can still be accommodating when combined with hypothetical and exploratory research.

Morrison et al. [20] have conducted an test ponder to compare the execution of standard and opened opening flowmeters with regard to weight drop, speed profile, and release coefficient. They found that the opened opening flowmeter had lower weight drop and higher release coefficient than the standard hole flowmeter, particularly at high Reynolds numbers, to measure the differential weight, inactive weight, and stream rate over both flowmeters for different stream

conditions and calculated the stream coefficient Cd for both flowmeters. the opened opening flowmeter was predominant to the standard hole flowmeter in keeping up its calibration over a wide extend of gulf stream conditions. The comes about and strategies were compared and, moreover assessed the metering characteristics of opening, spout, and venturi flowmeters, the execution of a opened hole flowmeter with four concentric rings of outspread openings, and a redress strategy for damp gas stream metering utilizing a standard opening and a opened hole flowmeter, separately. The likenesses and contrasts among the distinctive sorts of flowmeters, such as electromagnetic, mass, and turbine, were highlighted utilizing the comparison table from. The points of interest and drawbacks of utilizing opening and opened plate flowmeters, such as precision, rangeability, weight drop, fetched, and impact of thickness. In any case, the opened opening flowmeter is a promising elective to the standard opening flowmeter, but moreover distinguished the crevices and confinements of the existing writing and recommended headings for future inquire about, such as the impact of temperature, weight, and liquid properties on the flowmeter execution, the ideal plan of the opened hole plate, and the application of opened hole flowmeters in mechanical settings.

Shan, F. et al. [21] have conducted a consider that inspected the impact of the hole to pipe distance across proportion on the stream field behind a lean circular square-edged hole plate. This was done to degree the speed areas in a expansive range covering the reattachment locale. The analysts utilized a planar molecule picture velocimetry (PIV) framework with two side-by-side cameras. The calculations were based on the Navier-Stokes conditions. The center, distribution, and axisymmetric shear-layer locales were fittingly characterized, and the characteristic length and speed scales were decided in each locale. Particularly, the think about examined the impacts of the orifice-to-pipe distance across proportion, alluded to as the β proportion, on the stream field behind a lean circular square-edged opening plate. The boundary conditions set were no-slip at the dividers of the pipe and the hole plate. In spite of the fact that the run of flow-control parameters utilized in the consider was not expressly specified, the streamwise speed field for $\beta = 0.62$ and $Re = 25{,}000$ was utilized. The speed areas were measured utilizing a planar PIV framework and hence analyzed utilizing fitting factual strategies. In any case, it is worth noticing that the ponder has certain restrictions and presumptions. For occurrence, the utilize of a planar PIV framework may not be appropriate for capturing three-dimensional streams. Moreover, the ponder was conducted beneath particular conditions, which limits the generalizability of the discoveries to other scenarios. In any case, this think about gives a crucial premise for advance investigation in this field.

Boualem Laribi et al. [22] , have conducted a numerical experimentation of the conduct of the release coefficient and the impact of four punctured plates like stream conditioners on the release coefficient for stream estimation precision. The two transport conditions are utilized, one for the turbulence dynamic vitality k and the other for its scattering rate ε for the calculation. The stream is inspected with discuss at a Reynolds number of $Re=2.5x10^5$. the impact of hole meter distances across on the release coefficient for stream estimation. The stream is subject to two disturbers, specifically a 90° twofold twist in opposite planes and a 50% closed valve. The turbulent stream is inspected in a conduit with an inward distance across of 100 mm. The benchmarks ISO5167 and AGA3 stipulate that the blunder on the release coefficient Cd must be less than 0.5% for way better stream estimation exactness. By comparing their comes about with this condition, the creators found that the blunder gotten on the release coefficient with the four punctured plates is significantly decreased, particularly downstream station z = 25D (z =19D downstream disturbers). The blunders recorded by downstream disturbers are predominant to 12%. Downstream, with the punctured plates utilized independently, the blunders on the release coefficient are decreased to a esteem second rate to 1% for the four plates.

Junxia Gao et al. [23] have conducted an examination into the transitional stream characteristics of the two-stage hole and compared it with the single classic opening. The think about utilized hypothetical induction, computational liquid elements (CFD) recreation, and test estimation to investigate the transitional stream characteristics of the two-stage opening utilizing mineral oil. The Reynolds number extend considered was between 900 and 1700. The overseeing conditions utilized in the ponder were the Navier-Stokes conditions. The boundary conditions included an gulf speed extending from 0.5 to 2.2 m/s for the hole with a distance across of 3 mm, a weight of 1 bar at the outlet, and mineral oil with a thickness of 900 $kg/m^3$ and a kinematic thickness of 30 $mm^2/s$ at climatic weight. The numerical procedure utilized was the limited volume strategy. The ponder displayed the release coefficient and the weight drop over the two-stage opening. To guarantee the unwavering quality of the comes about, a comparison was made between the numerical and test information. The ponder concluded that the release coefficient of the two-stage opening is more prominent than that of the single hole beneath the same measurements, and the transitional stream state of the two-stage hole varies from that of the single hole. This consider gives profitable back for exact weight and stream control of the two-stage opening, and the part of the glory round and hollow gap can too serve as a important reference in the organized plan of micro-orifices.

Hollingshead et al. [24] have conducted a consider on the execution of Venturi, standard concentric hole plate, V-cone, and wedge stream meters in terms of their release coefficients at moo Reynolds numbers. The ponder utilized differential weight stream meters to examine the relationship between Reynolds number (Re) and release coefficients. In occasions where the streams had lower Reynolds numbers, it was accepted that they were laminar and subsequently, no turbulence demonstrate was utilized. For turbulence closure, the k-epsilon show was utilized. The overseeing condition utilized in the think about was the Bernoulli condition, which builds up a relationship between the weight drop over a stream meter and the stream rate. The ponder enveloped a run of stream controlling parameters, with the Reynolds number changing from 0.5 to 10,000. In arrange to conduct their inquire about, the creators utilized the Computational Liquid Elements (CFD) program Familiar as the numerical procedure, whereas GAMBIT was utilized as the preprocessing device to make the stream meter models. The creators concluded that as the Reynolds number approaches 1, the different stream meters display a quick decrease in their release coefficients.

Ding et al. [25] have attempted a Comparative Investigate try to examine the Pressure driven Characteristics of Three Sorts of Opening Plates in arrange to survey the scattering of vitality in hole plates that have diverse edges at a Reynolds number of $Re = 1.8 \times 10^5$. The $k - \varepsilon$ show was utilized to decide the vitality misfortune, divider weight, and the length of backflow for opening plates with sharp edges, square edges, and circular edges. The analysts utilized the Reynolds-averaged Navier-Stokes (RANS) conditions to mimic the stream field of the opening plates. The boundary condition consolidated the turbulent dynamic vitality of 0.0144 $u^2$ and the turbulent scattering rate $\varepsilon$ in = $k^{1.5}$ / 0.25D. The divider boundary was controlled by actualizing the divider capacities. Besides, the symmetric boundary condition was received, wherein the outspread speed on the symmetry hub was set to zero. The calculation burrow had a distance across of 0.21 m, an normal stream speed of 1 m/s, and a Reynolds number of $1.8 \times 10^5$. The analysts made an interesting finding that the hole plate with a sharp edge come about in the most noteworthy vitality scattering, while the square edged opening plate driven to the most reduced vitality scattering. Then again, the resistance to cavitation harm displayed the inverse slant for the hole plates.

S.H. Alvi et al. [26], have examined the misfortune characteristics of sharp-edged holes, quadrant-edged openings, and long-radius stream spouts for Reynolds numbers less than 10,000 and β proportions from 0.2 to 0.8. They consider classifying the stream into a completely laminar administration, a basic Reynolds number administration, a relaminarization administration, and a turbulent stream administration. The administering condition utilized was the vitality condition,

and the run of flow-control parameters utilized were the Reynolds number and β proportion. They utilized exploratory courses of action with weight taps, and the vulnerability gauges at 20:1 changes were included in the comes about. The numerical procedure utilized was extrapolating for Reynolds numbers more noteworthy than 10,000. Four oils with kinematic viscosities of 20 C, 350 C, 100 OS, and 10.5 t were utilized to cover the Reynolds number extend of 1 to 10,000. The think about displayed a variety of parameters such as release coefficient, misfortune coefficient, settling length, weight recuperation length, and middle line speed. They approved the comes about by comparing them with prior inquiries about, and they concluded that, for adequately moo Reynolds numbers, the misfortune coefficient is contrarily corresponding to the number and that, for tall β proportions, the relative impacts of grinding cause the Reynolds number to increment with β.

Naveenji Arun et al. [27], have conducted a comprehensive computational liquid flow (CFD) examination to explore the conduct of the release coefficient ($C_d$) in non-Newtonian streams through an opening meter. They included different concentrations of non-Newtonian liquids, and the beta proportions of 0.4, 0.6, and 0.8 were considered for each pipe breadth, which extended from 50mm to 200mm. The discoveries uncovered that the esteem of $C_d$ is complicatedly connected to the Reynolds number, and at the profoundly turbulent stream, it inevitably comes to an asymptotic state. Strikingly, when the Reynolds number surpasses 25000, the vacillation in the release coefficient becomes less articulated, and it accepts a steady esteem of around 0.6, adjusting with the built-up commercial benchmarks. Moreover, it was observed that the release coefficient showed an exponential increment as the Reynolds number raised from 100 to 10000. In this way, for consequent increases in the Reynolds number, the $C_d$ values remained consistent.

Mara Nilza et al. [28] have analyzed the discharge coefficient in hole plates by an exploratory and numerical examination. They found that a cone-shaped entrance hole plate is the most appropriate shape for stream estimation of thick liquids in which the Reynolds number is between 25 and 75, agreeing with the esteem of β. After a comprehensive examination, the ponder eventually concludes that if the impacts of dormancy are not accounted for when deciding the coefficient of inactive release, the coming values for said coefficient tend to be higher than at first expected. In arrange to conduct their examination, the analysts utilized the Navier-Stokes conditions as the overseeing conditions, whereas moreover consolidating both the no-slip condition and the coherence condition as the boundary conditions. Shockingly, the particular run of flow-control parameters utilized in the consideration is not expressly said inside the paper, taking off a little room for assist elaboration. In any case, it is worth noticing that the numerical strategies utilized

in the ponder were the profoundly respected Strategy of Characteristics and the Limited Volume Strategy, both of which are well-established and broadly acknowledged inside the field.

Hasana bulut et al. [29], have conducted a numerical arrangement to an unfaltering stream issue of a thick, incompressible liquid through a hole utilizing the Adomian decay strategy. They considered the relentless, two-dimensional movement of a thick liquid and utilized the Navier-Stokes conditions as the administering conditions. The no-slip condition at the dividers of the hole and the coherence of the stream at the channel and outlet of the hole were utilized as the boundary conditions. They approved their comes about by comparing them with the comes about gotten by other analysts and concluded that the Adomian deterioration strategy is a compelling and exact strategy for tackling the consistent stream issue of a gooey, incompressible liquid through an orifice.

Robert et al. [30] dig into the laminar stream elements of an incompressible liquid inside the entrance locale of a pipe, utilizing a numerical approach to accomplish a closer guess to the principal conditions of liquid movement than earlier thinks about. Utilizing a limited distinction walking method, the think encourages the assurance of speeds and weights at different pivotal positions inside the pipe, in this manner advertising a more exact arrangement by shunning linearizing suspicions and following the unique differential conditions of liquid movement. A comparative examination with past strategies uncovers noteworthy incongruities in comes about, especially with respect to speed profiles and improvement lengths, underscoring the predominance of the numerical approach. This investigation underscores the significance of precise arrangements in comprehending stream behaviors close pipe passages, significant for various designing applications. Hornbeck's work yields important bits of knowledge into laminar stream characteristics, particularly inside the channel locale, highlighting the need for thorough numerical arrangements grounded in the overseeing equations.

Şahin et al. [31] scrutinize the behavior of a laminar stream passing through a square-edged hole with movable thickness, pointing to observe the impact of opening plate thickness on stream characteristics. Utilizing numerical reenactments, the analysts dig into the stream behavior utilizing three-dimensional Reynolds-averaged Navier–Stokes conditions coupled with the k–ω shear-stress transport turbulence demonstrate, including an extend of opening plate thicknesses and breadths inside a pipe, with Reynolds numbers crossing from 2500 to 40,000. Their examination yields experience into parameters such as release coefficient, weight drop, and speed profiles, highlighting the considerable effect of square-edged hole plate thickness on stream behavior—a pivotal calculation for exact stream estimation and framework plan. Generally, Şahin

and Ceyhan's inquiry enhances understanding concerning laminar streams through square-edged openings with changing thicknesses, advertising profitable commitments to the field.

Đurđević et al. [32] investigate the behavior of single-hole opening (SHO) and multi-hole hole (MHO) gas stream meters through test and numerical examinations. Their investigation dives into comparing these two sorts of stream meters, exploring the mass stream and weight drop reliance in sticky discuss inside a 100 mm breadth conduit. Different multi-hole hole geometries with distinctive compression coefficients were inspected over a wide run of Reynolds numbers, with weight estimations taken both upstream and downstream of the opening. Also, they think about comparing the stream coefficient of a six-hole hole stream meter with that of an ordinary single-hole opening with the same withdrawal coefficient. Numerical recreations, utilizing computational equations suggested in the ISO 5167-2 standard for SHO stream meters, were conducted. The reenactments moreover consolidated an impediment at changing separations upstream from the hole to assess its effect on the measured weight drop, which comes about compared against exploratory information. The discoveries uncovered that the MHO stream meter displayed a lower particular weight misfortune coefficient and weight drop compared to the SHO stream meter. In any case, whereas illustrating prevalence, encouraging inquire is regarded as fundamental to building up the MHO stream meter as a practical substitution for SHO stream meters. In general, this ponder gives profitable experiences into the behavior of both single-hole and multi-hole opening gas stream meters, contributing to improved stream estimation precision and framework plan.

Jurga et al. [33] utilize different Reynolds-Averaged Navier–Stokes (RANS) turbulence models in numerical recreations to investigate turbulent stream through an opening plate at a Reynolds number (Re) of 23,000, with settled proportions of opening thickness-to-pipe breadth (t) and hole diameter-to-pipe distance across (β) at 0.1 and 0.5, separately. The fundamental objective is to survey diverse RANS models' execution concerning key stream parameters like weight drop, speed disseminations, and turbulence-concentrated profiles inside the pipe, comparing comes about against distributed exploratory information. The consider includes a few turbulence models, counting variations of the k – ε show family (like k – ε Moo Re, k – ε RNG, and k – ε Realizable), the k – ω SST (Shear Push Transport) demonstrate, the γ – SST (Gamma Shear Push Transport) demonstrate, and the EARSM (Express Arithmetical Reynolds Stretch Demonstrate). Key discoveries demonstrate that the k – ω SST, γ – SST, and EARSM models display great understanding with test estimations, outperforming the prescient capabilities of the k – ε show family, especially in perspectives basic for opening flowmeter plan. This investigate offers critical

experiences profitable for engineers and analysts included in upgrading stream estimation exactness and framework plan, especially in hole stream meter applications.

Zahra A S et al. [34], set out to plan and optimize a cavitating gadget through computational liquid elements (CFD) recreation. They are centered on a Venturi, famous for actuating hydrodynamic cavitation. The essential objective was to refine Venturi's geometrical setup to increase cavitation-induced decolorization of Congo ruddy colour. Different parameters such as joining point, dissimilarity point, throat length, and gulf weight were fastidiously surveyed. Utilizing both CFD recreation and exploratory techniques, the creators assessed the impacts of these parameters, utilizing reaction surface strategy (RSM) to pinpoint the ideal geometrical setup. Concurring with their CFD discoveries, particular parameters, counting the half point of the merging segment, throat length, and half point of the disparity area, were recognized as fundamental for maximizing the cavitation zone inside the Venturi. Ensuing experimentation uncovered that at a cavitation number ($C_v$) of 0.12, the outlined Venturi accomplished a surprising 38.8% decolorization of Congo ruddy colour, outperforming the execution of different hole plates tried. The think about underscores the viability of optimizing Venturi geometry in reinforcing the decolorization preparation, displaying its prevalence over conventional opening plates. Eventually, this inquiry presents critical experiences in upgrading the productivity of cavitating gadgets for color decolorization applications, pushing for the combined utilization of CFD recreation and test approval as a vigorous optimization approach for such systems.

Ning HE et al. [35] , have carried out an investigation of the proficiency of a hole vitality dissipator, utilizing hypothetical examinations and numerical reenactments as their apparatuses of examination. Their objective is to unwind the complicated components that impact the viability of this dissipator. Parameters scrutinized incorporate the Reynolds number (Re), the proportion of hole distance across to the internal breadth of the pipe (d/D), and the proportion of separations between holes to the internal breadth of the pipe (L/D). The pressure-driven characteristics experience outstanding changes as the stream navigates the opening, checked by sudden speed acceleration, increased turbulent vitality, and a diminish in weight, with turbulent vitality showing a spatial conveyance skewed towards higher values close to the pipe divider. Looking at single opening vitality dissemination setups, the creators watch a quick increment in the opening vitality scattering coefficient (K) with Re underneath 105, which stabilizes as Re outperforms this edge. They note parallel variety designs between K and the length of the distribution locale ($L_1$) concerning d/D proportions, with their work bends approximating straight lines. Transitioning to double opening vitality scattering arrangements, they discover that the moment opening ($K_2$)

shows a smaller vitality scattering coefficient compared to the, to begin with. Outstandingly, for dispersing between openings less than 5, K battles to fulfill its vitality dissemination work. Be that as it may, with a dividing surpassing 5, $K_2$ tends to stabilize, with negligible effect from the dispersing separate. The opening vitality dissipator is recognized for its focal points in optimizing venture formats, especially in hilly locales with space limitations, and for its adequacy in settling specialized challenges related to vitality dissemination. In conclusion, this investigation gives comprehensive bits of knowledge into the water-powered behavior of opening vitality dissipators, advertising profitable commitments to water-powered designing applications.

Stream estimation is an urgent handle over differing businesses, requiring an exhaustive comprehension of the vulnerabilities inborn in stream estimation procedures. Among these strategies, opening stream meters stand out for their common sense and broad selection. This audit by Sravani et al. [36] digs into the complexities of stream estimation elements utilizing hole plates, with a specific centre on scrutinizing the consequences stemming from varieties in the physical measurements of the opening. Central to the paper is an investigation of essential stream estimation standards, underscoring the ubiquity of opening stream meters in this space. The ponder fastidiously explores the impact of a few parameters on hole plate execution, enveloping variables such as the thickness of the opening plate, orifice-hole breadth, number of gaps, sort of liquids, and the position and sort of the plate. Leveraging Computational Liquid Flow (CFD) reenactments, the creators approve the impacts of these parameters, saddling CFD's capability to reveal the energetic behavior of opening plates. The viable suggestions of this investigation are significant; a nuanced understanding of these parameters is considered basic for accomplishing exact stream estimation results. Industry specialists stand to advantage essentially from this information, as it engages them to fine-tune opening plate plans, in this manner optimizing stream estimation forms. In quintessence, this audit sheds comprehensive light on the multifaceted domain of stream estimation utilizing hole plates, underscoring the basics of considering different parameters to guarantee the unwavering quality and accuracy of estimation results.

Suat C et al. [37], have conducted a study, on the behavior of flow-restricting gadgets, especially openings and capillary tubes, when subjected to shaky stream conditions at Reynolds numbers. These gadgets, characterized by their little breadths, play an essential part in different applications, thus justifying a nitty gritty examination of their execution. The essential objective of the investigation was to find out the stream coefficients of both holes and capillary tubes inside the indicated moo Reynolds number extend of 10 to 650. Through test requests, analysts scrutinized the stream characteristics of holes and capillary tubes traversing breadths from 0.35 mm to 0.70

mm, stamping a flight from predominant writing which transcendently centers on relentless streams at direct to tall Reynolds numbers. A key comparison developed between capillary tubes and holes, uncovering that capillary tubes display predominant capillarity properties with regard to holes of proportionate breadth. Advance examinations revealed that adjustments in the proportions of the capillary tube length to the breadth and opening breadth to pipe breadth impact the throttling or limiting properties of both gadgets. Outstandingly, whereas capillary tubes bring about higher weight misfortunes, they too illustrate utility as pressure-driven aggregators in controlling flow-induced vibrations. The ponder portrayed that as the proportion of opening breadth to pipe distance across increments and the proportion of capillary tube length to distance across diminishes, higher stream coefficients are accomplished. Furthermore, the move from gooey to inertia-controlled stream shows at lower Reynolds numbers for smaller holes with tall distance across proportions and capillary tubes with decreased length-to-diameter proportions. In quintessence, this inquiry gives profitable experiences into the behavior of flow-restricting gadgets beneath moo Reynolds number conditions, explaining the refinements between capillary tubes and orifices.

Araoye et al. [ 38] have considered the complexities of stream elements through a consecutive setup comprising two associated bevel-edged opening plates arranged inside a flat pipe of 25.4 mm inner distance across. Utilizing computational liquid flow (CFD) with the realizable k-ε vortex thickness demonstrate, the creators scrutinized different viewpoints of stream behavior. The examination centered on key parameters, counting pipe stream speed extending from 1 to 4 m/s, hole dividing of 1D and 2D, and opening plate breadth proportions of 0.5, 0.63, and 0.77. All through the think about, turbulent stream won, characterized by Reynolds numbers extending from Re = 2.54 × 104 to 1.02 × 105. Eminently, the position of the vena contracta related the to begin-with hole remained unaffected by the expansion of a moment hole but changed with opening breadth proportions. Downstream of the moment opening, the nearness of vena contracta was unexpected upon hole dispersing. Stream designs between the holes and downstream show similitude to single hole stream, including distribution, reattachment, and shear layer locales. In any case, unmistakable stream marvels rise in the dispersing between the openings, counting a donut-shaped vortex close to the divider and a jet-like stream in the center locale. The ponder encouraged illustrated the impact of hole dispersing on add up to weight drop and water-powered misfortunes, with 1 and 2 pipe distance across spacings coming about in the most elevated and least weight recuperation, individually. These discoveries bear viable noteworthiness, and advertising experiences into weight control strategies without requiring a total update of the

stream framework. In quintessence, this investigate lights up the behavior of multi-stage limiting openings, underscoring their effect on stream characteristics and weight losses.

Fluid stream through hole plates stands as a significant component in stream estimation over differing businesses, where opening meters appreciate far-reaching utilization owing to their shortsighted plan, cost-effectiveness, and operational ease. Inside this setting, C. R. Sanghani et al. [39] attempted an examination into the repercussions of changing hole geometries on weight drop, utilizing Computational Liquid Flow (CFD) methods. The essential point was to scrutinize liquid streams through opening plates with distinctive geometries, with a particular center on distinguishing the geometry coming about in negligible weight misfortune. ANSYS CFX 15.0 program encouraged CFD reenactments, wherein different hole plate setups were inspected concerning weight drop. Six particular geometries were beneath thought, counting square-edged and square-edged with a 45° back-cut, among others. Strikingly, beneath indistinguishable conditions of breadth proportion and thickness, the opening plate with a 45° back-cut displayed the most elevated weight misfortune, though the streamline approach hole plate illustrated the most reduced weight misfortune. These discoveries bear down-to-earth noteworthiness, advertising direction for selecting the most suitable hole plate geometry in real-world stream estimation applications. In pith, this investigation contributes profitable experiences into the behavior of distinctive hole geometries concerning weight drop, subsequently encouraging engineers and professionals to optimize stream estimation frameworks.

Prabhata K. et al. [40] introduce a novel high-accuracy explicit equation for calculating the discharge of circular sharp-crested orifices. Traditionally, obtaining such discharge values relied on experimental data for the discharge coefficient, which could introduce errors during graph reading. The newly proposed equation offers an analytical approach that integrates both viscous and potential flow effects, promising enhanced accuracy. The classical discharge equation for circular orifice flow from the side of a large tank served as the foundation, where the discharge ($Q$) is determined by the discharge coefficient ($C_d$), orifice diameter ($d$), gravitational acceleration ($g_g$), and depth of the orifice centre below the free surface ($h$). The variation of the discharge coefficient ($C_d$) with a term involving the kinematic fluid viscosity ($n$) was explored by Lea (1938) and further analyzed by Rouse (1946). Their investigations provided insights into the relationship between $C_d$ and the term

$$\left(\frac{d\sqrt{gh}}{n}\right)^{\frac{1}{2}} \tag{1.1}$$

offering curves based on average orifice flow velocity. The authors' explicit equation for the orifice discharge integrates these findings, presenting a formula that accounts for both viscous and potential flow effects. This equation,

$$Q = 0.7 * C_d * \left(1 + \sqrt{1 + 1.43\frac{n}{dgh}}\right) \quad (1.2)$$

offers a more precise prediction of discharge compared to traditional methods. Overall, the work enhances the understanding of circular sharp-crested orifice flow and provides a refined equation with practical applications in mind.

Stream estimation is a critical undertaking for several organizations, which sometimes rely on hole plates for precise valuation. In this study, Malatesh Barki et al. [41] investigate the liquid components of single-hole and multi-hole hole plates using computational liquid flow (CFD). With water serving as the working liquid, the analysis examines how gap-opening behavior affects stream properties. The analysts employed Hyper Work 11.0 for fitting, and CATIA V5 R20 for constructing the pipe regions and opening plate geometry. We used ANSYS Familiar 6.3.26 to investigate the stream. We examined parameters such as non-standard opening plate design circumstances. We examined four distinct width proportions across various configurations, ranging from single-hole openings to those with sixteen gaps. The investigator examined the stream rate, weight drop, speed, and turbulence-focused flow while maintaining a consistent internal pipe breadth of 50 mm and a dependable plate thickness of 3 mm. The study reveals that multi-hole hole plates display more common stream characteristics than their single-hole counterparts with similar take off ranges. Interestingly, the process or delivery of the hole gaps significantly influenced the overall performance. These discoveries provide commonsense suggestions, empowering engineers and specialists to optimize opening plate plans tailored to specific applications. In essence, this investigation contributes important bits of knowledge to the behavior of both single-hole and multi-hole opening plates, underscoring the basic part of the gap course of action in stream estimation applications.

Gianpietro Di Rito et al. [42] dive into the complexities of liquid stream through a four-way servo valve, with a particular center on hole stream flow. The servo valve stands as an essential component inside water-powered frameworks, especially in aviation applications, where an exact understanding of stream characteristics inside the openings is basic for exact modelling and execution forecast. Key discoveries show that opening release productivity depends on stream conditions, and there are differences between turbulent, mixed, and laminar stream conditions. Eminently, the classical approach, accepting turbulent streams through servo valve holes, can lead

to mistakes, particularly in extraordinary conditions experienced in aviation actuators. The study aims to achieve two main objectives: understanding the transition from laminar to turbulent flow and promoting a new approach to enhance hole release efficiency in mixed flow conditions. To better understand the behavior of the opening stream, the authors' method makes use of the Moog D633 four-way servo valve and incorporates educated guesses and computational fluid flow (CFD) simulations in the STAR-CD environment. Considering stream conditions and utilizing Reynolds-dependent opening conditions is crucial, particularly in aviation applications where unexpected phenomena such as high checking loads or moo speeds can occur. These factors can result in the need for laminar or blended stream designs in servo valve openings. In general, this study provides valuable insights into the behavior of hole streams in four-way servo valves. Stream condition analyses and accurate modelling methods are crucial for precise execution prediction.

Saeed Ahmed et al. [43] have considered Multi-stage holes (MSOs) to be fundamental components of different businesses, serving in applications such as oil refineries, atomic control plants, and chemical offices, where they play a vital part in weight diminishment. Be that as it may, this decrease frequently accelerates cavitation—a marvel characterized by the arrangement of vapor bubbles due to weight drop. Critical obstacles associated with cavitation include disintegration, unwelcome vibrations or disturbances, and misfortune in practice. It becomes essential to comprehend cavitation to handle these problems. This study's primary goal is to suggest a design modification for mechanical multi-stage holes aimed at reducing the start of cavitation. Utilizing the Computational Liquid Elements (CFD) examination, the analysts reenacted a three-dimensional setup of a six-stage opening, with cavitation happening after the final organize. Approval of the CFD demonstration was conducted by comparing it with real-time plant information beneath genuine working conditions. Critical discoveries arose from testing different adjustments in hole geometry, with specific accentuation on gap introduction inside the openings. The objective was to dispense with cavitation issues related to the existing geometry. The multi-holed design, which had four gaps in each opening plate coordinated at alternate places, proved to be the most effective of the attempted setups. This modified shape eliminated cavitation effects under the same operating circumstances. In conclusion, this way of thinking equips useful information to predict cavitation in mechanical multi-stage holes through astute plan modifications, thus improving the efficacy and dependability of the framework.

The think-about performed by Xueping Gao et al. [44] dives into the complexities of stream flow inside a vertical pipe inlet/outlet including an anti-vortex plate, an arrangement commonly sent in

pumped capacity plants. Given the complexity of the two-directional stream in such frameworks, accomplishing ideal pressure-driven conditions presents a noteworthy challenge. To investigate stream behavior across various redirection opening statures and dissimilarity points, the authors performed numerical recreations using the realizable k-ε turbulence show. The investigation focused on head mishaps and speed distribution inside the vertical pipe inlet/outlet, examining pressure-driven circumstances for the pumping and producing modes. Remarkably, the analysis revealed that it was difficult to achieve optimal water-powered conditions simultaneously for both modes. The study suggests updated value ranges for preoccupation hole height and uniqueness points to improve framework efficiency and security. These ranges consider factors like head mishaps, the highest speed at redirection openings, and the height of the inverted stream zone. Essentially, this study provides useful information for optimizing pressure-driven conditions in pumped capacity plants by elucidating the stream's behavior in a vertical pipe fitted with an anti-vortex plate.

Michael et al. [45] highlight the vital role of hole plates in stream estimation over different mechanical settings, emphasizing their cost-effectiveness, unwavering quality, and effortlessness. However, they note that defilement from substances such as oil or pipeline slime can antagonistically influence the release coefficient, which is critical for exact stream assessment. To investigate this, the study examines the effect of defilement on opening plate execution, using both exploratory tests and computational liquid elements (CFD) recreations. We mimicked real-world defilement in the tests by connecting circular metal plates to the hole plates and conducted a comparative investigation of the CFD recreations. The findings demonstrate that the change in the release coefficient is dependent on the defilement thickness relative to the opening edge. We determined a condition with an instability of 0.28% to gauge the rate of change in the release coefficient. Moreover, the study's findings demonstrated reliability with the ISO/TR 12767 rules, suggesting the inclusion of the modern demonstration in future standard corrections. This inquiry improves our understanding of contamination's impact on opening plate execution, highlighting the importance of exact modelling and estimation in mechanical applications.

Mara N. E.'s et al. [46] study delves into the intricacies of incompressible pulsating streams through hole plates, focusing on situations with low Reynolds numbers. Opening plates, which are important for stream estimation, require close inspection under turbulent stream conditions to ensure accurate estimates. The word "throbbing stream" refers to a typical occurrence in mechanical settings, which is defined as sporadic variations in liquid movement. The authors' test procedures explained the effects of worldly inactivity and throb varieties on the release coefficient.

Beyond conventional methods, the analysis specifically considers fluid flow in small-diameter channels, where Reynolds numbers remain low. It is impossible to overstate the practical implications of knowing how pulsating stream influences hole plate execution since reliable stream estimate provides the backbone of many mechanical structures. The insights gained from this investigation not only help to optimize hole plate designs but also assure raising estimation accuracy. The behavior of an incompressible pulsating stream via opening plates is illuminated in summary by this study, highlighting the significance of accounting for different Reynolds numbers in practical applications.

K. Roul et al. [47] have conducted a crucial study in stream estimation by analysing the behavior of one- and two-phase streams via lean and thick gaps inside planar channels in this work. Opening plates are widely used in stream estimate applications, and it is essential to have a thorough grasp of how they operate under various stream conditions to ensure accurate calculations. Utilizing computational liquid flow (CFD) calculations utilizing the Eulerian–Eulerian demonstration, the consider fastidiously surveys weight drops over openings. Working conditions envelop gas and fluid shallow speed ranges, covering a breadth from 0.3 to 4 m/s for gas and 0.6 to 2 m/s for fluid. Recreations for single-phase streams focus on the water stream to determine the release coefficient and the two-phase neighbourhood multiplier, which are essential for replicating weight reductions in scenarios involving two-phase streams. The researcher encourages further investigation into the impact of opening geometry by considering various characteristics, such as zone proportions, hole plate thicknesses, and inward channel distances counted. Numerical documents are thoroughly approved against exploratory information sourced from existing writing. In outline, this inquiry yields important experiences into the behavior of streams through lean and thick holes in flat channels, underscoring the need to consider assorted stream conditions and opening geometries for exact stream estimation applications.

K. Roul et al. [48] explore the turbulent flow of streams in a square-sectioned channel with a 90° square elbow through experimental methods. The researchers strategically placed circular turbulators near the inner radius of the elbow wall to minimize pressure loss within the ducting system. The experimentation included a range of Reynolds numbers from $1.6\times10^4$ to $9.5\times10^4$, as well as different average flow speeds of 2 m/s, 6 m/s, and 12 m/s. We strategically placed turbulators at intervals of 5°, 10°, 15°, and 20° along the inner walls. The findings showed a noticeable increase in turbulence intensity near the inner radius wall of the elbow when using $C_T$. In addition, the ducting with $C_T$ generally showed higher levels of turbulence compared to the ducting without $C_T$ .Significantly, the incorporation of $C_T$ resulted in a decrease in pressure loss

throughout the ducting, especially at Re values of $1.6\times10^4$ and $4.8\times10^4$, and when $C_T$ was placed at $\alpha=10°$, 15°, and 20°. Unfortunately, at $Re=9.5\times10^4$, the installation of the $C_T$ did not succeed in reducing the pressure drop. However, regardless of the $\alpha$ values used, $C_T$ placement often results in a reduction in pressure drop within the ducting. This study shows how circular turbulators might help lower pressure losses in ducting systems with elbows. This gives us useful information for making fluid flow better in these setups.

In this paper, the makers named Katharina Schrank et al. [49] challenge the customary one-dimensional approach to reenacting fluid control systems, which routinely disregards the closeness of entrained examination, driving to vital botches. They address this restriction by analysing the classical opening condition, at first decided on Bernoulli's condition, and open it to oblige a minute scattered vaporous organize. Examining how laminar, turbulent, or laminar-to-turbulent move stream ranges behave in these kinds of situations is crucial. The study evaluates both single-phase and two-phase streams via a weight-driven hole using Computational Liquid Stream (CFD) tools. It focuses on computing and contrasting release coefficients fundamental to the hole condition. Test underwriting of these excitements is conducted utilizing a late characterized test arrangement, which locks in the estimation of both one-phase and two-phase streams. The roughly shed light on the complex stream of the two-phase stream inside water-fueled openings, advancing useful bits of data through the comparison of calculated, reenacted, and measured information. By and huge, this ask around inside and out moves our understanding of how entrained talk about impacts weight driven gap stream, emphasizing the requirement of joining two-phase impacts in fluid control systems diversions to overhaul precision and faithful quality. This study roughly delves into the analysis of a six-hole gap stream meter using a combination of numerical simulations and exploratory approaches. Examining the basic stream properties in a multi-hole opening stream meter configuration is the main goal. Test examinations were carried out on sticky discuss inside a channel measuring 100 mm in distance across. The comes about revealed that the multi-hole opening meter caused less weight misfortune compared to its single-hole partner, credited to early stream reattachment wonders. Moreover, Computational Fluid Stream (CFD) amusements affirmed the exploratory disclosures, fortifying the faithful quality of the observed comes about. In pith, this ask-around basically contributes to the comprehension of the operational components of multi-hole gap stream meters, publicizing imperative bits of information into their execution characteristics.

The author K H Yau et al. [50] thinks about dive into looking at the weight drop execution of a thick plate limitation opening over different opening proportions. The fundamental objective is to

evaluate how distinctive hole proportions (ϕ) influence weight drop execution, utilizing the ANSYS program for numerical reenactments. The strategy utilized ANSYS Familiar to show the confinement hole, changing opening proportions from 0.5 to 0.75, with stream speeds extending from 50 to 420 m/s, while considering the hydrocarbon vapor stage. The results disclosed reliable patterns in release coefficients compared to existing writing and hypothetical values. Outstandingly, an exponential increment in weight drop execution was watched with an expanding Reynolds number (Re). At tall Re ($8.75\times10^6$), the weight drop surged by 63% from the pattern (Re = $1.08\times10^6$) for ϕ = 0.75. Especially for hydrocarbons with moo rheological properties and tall Re, a ϕ of roughly 0.75 comes about in a weight drop of 0.18 MPa. In pith, this investigation offers profitable knowledge into optimizing thick plate confinement holes to relieve weight drop.

In this study, the author D Zahariea et al. [51] comparison between the eccentric and conventional concentric orifice plates for liquid flow measurement is investigated. The primary goal is to assess the liquid's strong particle sedimentation propensity using an oddball hole plate. One of the strategies is using the ANSYS Familiar program to perform numerical research. This involves many stages, including creating a three-dimensional strong demonstration, freeing up the liquid space, coinciding, defining boundary constraints, choosing a turbulence display, comprehending computations, and establishing meeting requirements. The comes about highlights particular contrasts between the two sorts of hole plates. With the concentric opening plate, isolated stream districts are watched both upstream and downstream, showing potential sedimentation ranges for strong particles. Then again, the unpredictable opening plate shows a streamlined design recommending a negligible chance of sedimentation due to the nonattendance of isolated streams at the foot of the pipe. In general, this thinks about offers critical experiences into the behavior of unconventional opening plates, especially in the setting of stream estimation applications.

## 1.4 Summary of this literature review

In this review, an attempt has been made to analyze the fluid flow characteristics through orifice plates in various industrial applications, considering different flow conditions and orifice geometries. Studies focus on single-phase and two-phase flow through thin and thick orifices, exploring pressure drops in horizontal pipes under various gas and liquid velocities. Flow characteristics and patterns are depicted in terms of pressure drops, velocity profiles, and hydraulic losses, as discussed in the results and discussion sections. These flow characteristics are studied across different geometries, including rectangular and bevel-edged orifices, under Reynolds numbers ranging from $10^3$to $10^6$. The governing equations for the conservation of mass and momentum are discretized using computational fluid dynamics (CFD) techniques. The discretized

equations are solved iteratively to analyze flow behavior and pressure losses. From the numerical investigations, it has been observed that variations in orifice geometry significantly impact pressure drops and flow patterns. Research on multi-stage orifices addresses cavitation, showing that modifying orifice geometry can mitigate these effects, enhancing system reliability. Low Reynolds number studies highlight differences in flow coefficients and pressure losses between orifices and capillary tubes. Overall, a detailed examination of orifice plate geometries, flow conditions, and potential issues like cavitation ensures precise and reliable flow measurements, contributing significantly to the optimization of industrial processes. Validation of these numerical simulations is performed against experimental data, demonstrating the robustness of the CFD approach.

## 1.5 Problem Identification

The journal provides a thorough exploration of recent progressions within the realm of numerical analysis, square edge orifice plate array of fluid flow. Most of these studies were based on investigating the effect of the orifice thickness at different Reynolds numbers. In the previous studies, the effects of different $\beta$ have not been extensively studied. The numerical simulations to determine the discharge coefficients are validated in the above-mentioned literatures, but no comprehensive study has been performed to investigate the effects of different orifice characteristics on the flow fields. This allows investigation of a variety of different orifice characteristics in both laminar and turbulent regimes and improves the knowledge of, how these characteristics affect the behavior of the flow through the orifice. however, there is some limited universal standard of single-hole orifice that exists in the world today. Thus, the investigation of geometric parameters that control the performance of single-hole orifices is an active area of research. Also, there is a lack of parametric investigations of these geometrical parameters, and their interaction effect is not fully explored hitherto. This study is an attempt to enrich the literature with a new design of single-hole orifice and to explore its functionality using CFD modeling. This research aims to optimize the geometrical parameters which affect the performance of single-hole orifice plates. The pressure loss coefficient is selected as the performance parameter in this study, which is a measure of pressure loss caused by the orifice plates in a conduit. Moreover, flow conditioning characteristic of the single-hole square edge orifice plates is also analyzed in terms of flow development length, downstream of orifice plates.

## 1.6 The objective of the Present Research

The scheme of the proposed research work is focused as follows.

- To analyze the axial velocity profiles for the square edge orifice plate near the throat and the restriction at radial locations under turbulent flow conditions (low and high Reynolds number).
- To understand the effects of design and position of central restriction placed in an orifice plate.
- To represent the streamlined contours of orifice plates with geometrical restrictions varying the Reynolds number and β ratio to observe the recirculating bubble zones, jet flow, and vena contracta.
- To represent the pressure contours of orifice plates with geometrical restrictions varying the Reynolds number and β ratio to observe the pressure distribution effects.
- To Examine how varying the size of orifice holes (β ratio) and the Reynolds numbers influence the axial velocity, and turbulence flow characteristics such as turbulent kinetic energy, and dissipation rate.

# CHAPTER 2

## COMPUTATIONAL FLUID DYNAMICS & MATHEMATICAL FORMULATIONS

### 2.1 Fluid Dynamics (CFD)

A detailed introduction to Computational Fluid Dynamics and the CFD code Ansys 2024 are presented in the present chapter. Using numerical simulations and constantly updated codes, computational fluid dynamics (CFD) is a powerful technique that provides a qualitative forecast of a flow field. Aerodynamics research was the first use of computational fluid dynamics (CFD), but it swiftly expanded to other engineering domains, including marine and offshore technologies. Over time, researchers have produced several CFD codes, both licensed and open source. Nonetheless, almost all CFD algorithms use the same three-step process to solve problems:

- **Initial processing**: pre-processing includes establishing the physical parameters, boundary conditions, and geometries, and creating a computational domain mesh.
- **Resolving**: The CFD programs' relevant solvers are chosen to tackle the problem. The flow variables included in nodes within a cell in the pre-defined mesh are computed by the solver.
- **After processing**: Various post-processing tools are used to process the numerical findings. Processing the output data for flow variables or displaying the flow are two possible uses for this.

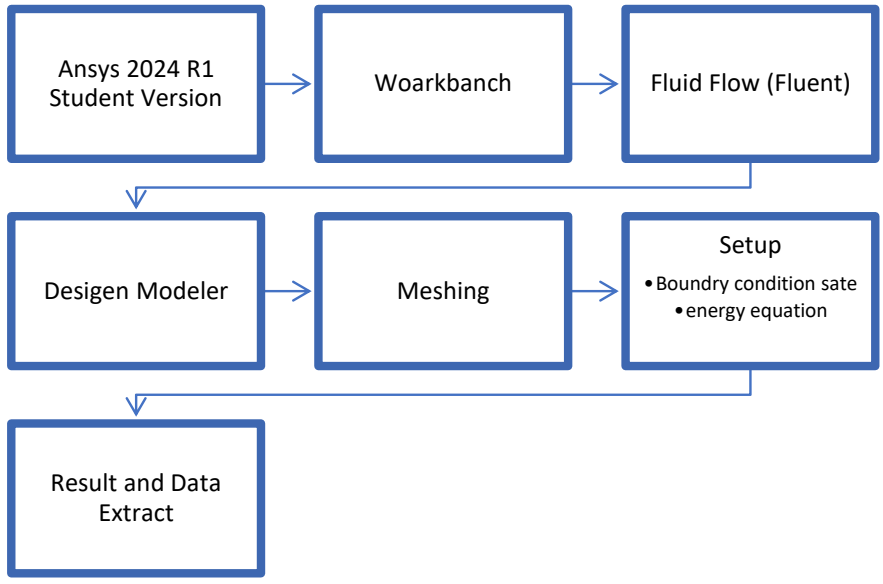


*Figure 2 Process of Ansys work.*

## 2.2 Computational domain

The computer models in Figures 1, 2, 3, 4, and 5 show the computational domain for turbulent flow through a rigid asymmetric 2D model of a square-edged orifice inside the pipe and a modified orifice plate with different orifice hole diameters (d). The external dominance idea is taken from Manish et al. (2012), and this current research also validates the paper. For the modified geometrical modelling of the orifice and the pipe. The inlet pipe length is 20 mm and the out length pipe length is 180 mm and, all the diameters are in Table 1. The flow is considered as two-dimensional, turbulent, and symmetric about the axis. The fluid is assumed to be incompressible and follows Newtonian laws.

The Beta Ratio (β) is a crucial parameter in orifice plate design, defined as the ratio of the orifice bore diameter to the pipe's inner diameter. Per the ISO 5167-2 standard, the Beta ratio should ideally be between 0.15 and 0.7. However, this range can vary slightly depending on specific applications and conditions.

For the β calculation: $\beta = \frac{d}{D}$ (Eq. 1)

where d is the orifice diameter and D is the pipe diameter.

**Geometry Details and Boundary Conditions:**

| Reynolds number | Fluid Density (kg/m³) | Diameter of pipe (D) (m) | Orifice diameter (m) | Thickness Of orifice (t) in (m) | Dynamic Viscosity (kg/ms) | β ratio | Velocity for β ratio (m/s) |
|---|---|---|---|---|---|---|---|
| 6859 | 998.2 | 0.0126 | 0.00433 | 0.00345 | 0.001003 | 0.34325 | 0.5469 |
| 6859 | 998.2 | 0.0126 | 0.00553 | 0.00345 | 0.001003 | 0.43849 | 0.5469 |
| 6859 | 998.2 | 0.0126 | 0.00673 | 0.00345 | 0.001003 | 0.53373 | 0.5469 |
| 6859 | 998.2 | 0.0126 | 0.00793 | 0.00345 | 0.001003 | 0.62897 | 0.5469 |

*Table 1 Computational Domain Table for beta ratio*

| Reynolds number | Fluid Density (kg/m³) | Diameter of pipe (D) (m) | Orifice diameter (m) | Thickness Of orifice (t) in (m) | Dynamic Viscosity (kg/ms) | Velocity (m/s) |
|---|---|---|---|---|---|---|
| 3375 | 998.2 | 0.0126 | 0.004325 | 0.00345 | 0.001003 | 0.26915 |
| 6859 | 998.2 | 0.0126 | 0.004325 | 0.00345 | 0.001003 | 0.54698 |
| 12167 | 998.2 | 0.0126 | 0.004325 | 0.00345 | 0.001003 | 0.97028 |
| 19683 | 998.2 | 0.0126 | 0.004325 | 0.00345 | 0.001003 | 1.56965 |

*Table 2 Computational Domain Table for Reynolds numbers*

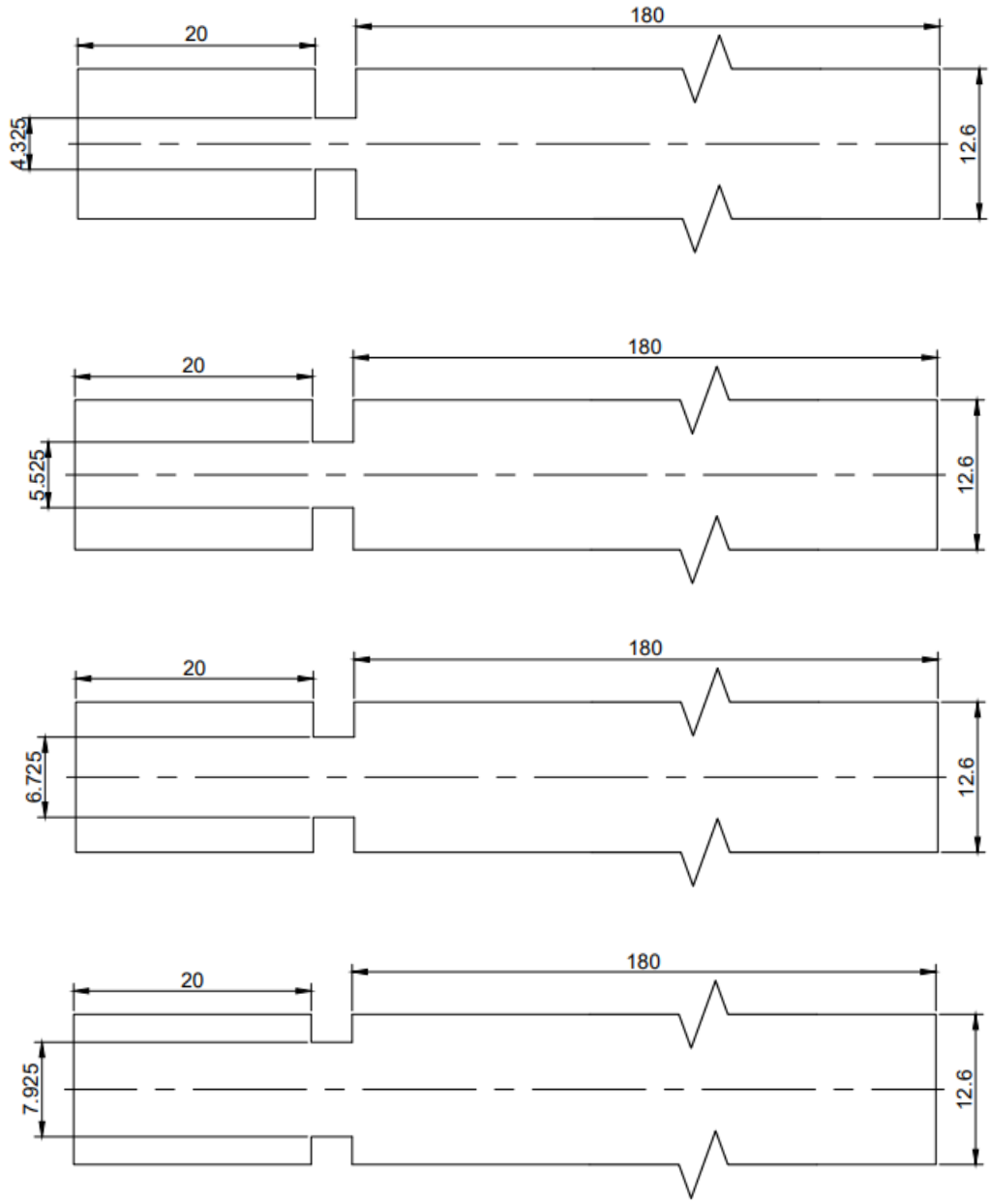


*Figure 3 Computational domain of modified orifice, circular hole secure edge cavity*

## 2.3 Working principle of orifice meter

The orifice meter is a plate with a sharp-edged hole in the middle, concentrically placed inside a pipe perpendicular to the flow direction. The pressure difference measured by the pressure tapping on the upstream and downstream sides of the flow is combined with Bernoulli's equation to obtain the flow rate.

- Mass balance:

$$\dot{Q} = A_1 V_1 = A_2 V_2$$
$$V_1 = (\frac{A_2}{A_1}) V_2 \quad \text{(Eq. 2)}$$

- Bernoulli's equation:

$$\frac{P_1}{\rho g} + z_1 + \frac{V_1^2}{2g} = \frac{P_2}{\rho g} + z_2 + \frac{V_1^2}{2g} \quad \text{(Eq. 3)}$$

- The equation can express the volumetric flow

$$Q_{theoretical} = V_2 A_2 = \frac{A_2}{\sqrt{1-\beta^2}} \sqrt{\frac{2g*(p_1 - p_2)}{\rho g}} \quad \text{(Eq. 4)}$$

Where, the diameters of the pipeline and the orifice hole, $p_1$ and $p_2$ are upstream and downstream pressures, then the flow rate can be obtained using the above equation by measuring the pressure difference $(p_1 - p_2)$. The β ratio between orifice diameter and pipe diameter. is assumed to have no pressure loss, which is unrealistic as pressure loss due to frictional effects is inevitable. As a result, $V_2$ is overpredicted

## 2.4 Governing Equations for Turbulent Flow

The present study assumes that the flow is incompressible and viscous. The governing equations used by the CFD code Fluent flow:

- continuity equation or the conservation of Mass Equation for two-dimensional incompressible flows:

$$\frac{\partial \rho}{\partial t} + \frac{\partial(\rho u)}{\partial x} + \frac{\partial(\rho v)}{\partial y} + \frac{\partial(\rho w)}{\partial z} = 0 \quad \text{(Eq. 5)}$$

- Navier Stokes Equation or the conservation of Momentum Equation for two-dimensional incompressible flows.

$$\rho \frac{du}{dt} = \rho g - \frac{\delta p}{\delta x} + \mu \left( \frac{\delta^2 u}{\delta x^2} + \frac{\delta^2 u}{\delta y^2} + \frac{\delta^2 u}{\delta z^2} \right) \quad \text{(Eq. 6)}$$

$$\rho \frac{dv}{dt} = \rho g - \frac{\delta p}{\delta y} + \mu \left( \frac{\delta^2 v}{\delta x^2} + \frac{\delta^2 v}{\delta y^2} + \frac{\delta^2 v}{\delta z^2} \right) \quad \text{(Eq. 7)}$$

In the case of turbulent flow, the equations need to be solved depending on the turbulence model that is used in the computational analysis. The standard k-ε model is used in the simulations carried out, one for k (turbulent kinetic energy) and one for ε (rate of viscous dissipation).

$$\begin{aligned} \frac{\partial(\rho k)}{\partial t} + div(\rho k U) &= div\left[\frac{\mu_t}{\sigma_k} grad\, k\right] + 2\mu_t S_{ij} S_{ij} - \rho\varepsilon \frac{\partial(\rho\varepsilon)}{\partial t} div(\rho\varepsilon U) \\ &= div\left[\frac{\mu_t}{\sigma_\varepsilon} grad\, \varepsilon\right] + C_{1\varepsilon} \frac{\varepsilon}{k} 2\mu_t S_{ij} S_{ij} - C_{2\varepsilon} \rho \frac{\varepsilon^2}{k} \end{aligned} \quad \text{(Eq. 8)}$$

Where the eddy viscosity is : $\mu_t = \rho C_\mu \frac{k^2}{\varepsilon}$

## 2.5 Numerical Methodology

In our computational fluid dynamics (CFD) recreations, we changed the channel velocity according to Reynolds numbers extending from $15^3$ to $27^3$, considering water as fluid for this investigation at room temperature. For the inlet pressure, it was reliably set to zero, and ANSYS-Fluent was utilized to illuminate the overseeing conditions beneath steady-state conditions. The Semi-Implicit Pressure Linked Equation (SIMPLE) algorithm helped us solve all the discretized equations and made sure that everything converged when the residuals fell below $10^{-6}$. Pressure measurements, taken as area-weighted averages at a specific pipe surface 2D from the inlet, provided critical data. Several turbulence models were looked at, the k-epsilon model was chosen because it was easier to compute and more accurate at predicting flow patterns far from boundaries. On the other hand, the K-epsilon model performed better near walls. Our investigation included a series of simulations using an orifice meter with a throat diameter variable according to the β ratio ranging of $0.3432$ to $0.6289$ and a length of 3.45 mm. The upstream stream length was set to 20 mm, with the pipe diameter is 12.60 mm, guaranteeing adequate lengths upstream and downstream of the opening plate to relieve boundary condition impacts and advance the completely created turbulent stream. The k-epsilon turbulence demonstration was chosen for its adjustment of precision and computational effectiveness, with second-order numerical exactness connected. Understanding all discretized conditions in an isolated way utilizing the basic calculation, we found our computed values to adjust closely with standard values, inside a vulnerability restraint of 0.6% as per ISO-5167-2 measures, thus approving our computational approach. Utilizing the limited volume procedure, discretization plans included second-order plans for weight, the basic conspire for pressure-velocity coupling, and second-order upwind plans for energy, kinetic energy (k), and turbulence dissemination rate (ε), underscoring the strength of our technique.

## 2.6 Meshing study

In the present study we used a two-dimensional structured mesh containing rectangular elements. We optimize the number of elements by conducting a grid independence study. There may be some errors in the final solution due to the grid's coarseness. So, a grid independence study is necessary for the analysis of any CFD problem using the software package Ansys. That’s why we employed an unstructured mesh to set up the orifices determined the mesh density through a grid-independence study and used the meshing tool in the ANSYS 2024 R1 Student Version to create the mesh. Mesh applications employ a 2D hexahedral block-structured mesh to discretize all models across the entire computational domain. We have defined an inflation mesh property with

5 layers to properly resolve the boundary layer along the fluid domain walls and around the orifice plate and adjusted the thickness of the first layer for the dimensionless wall distance.

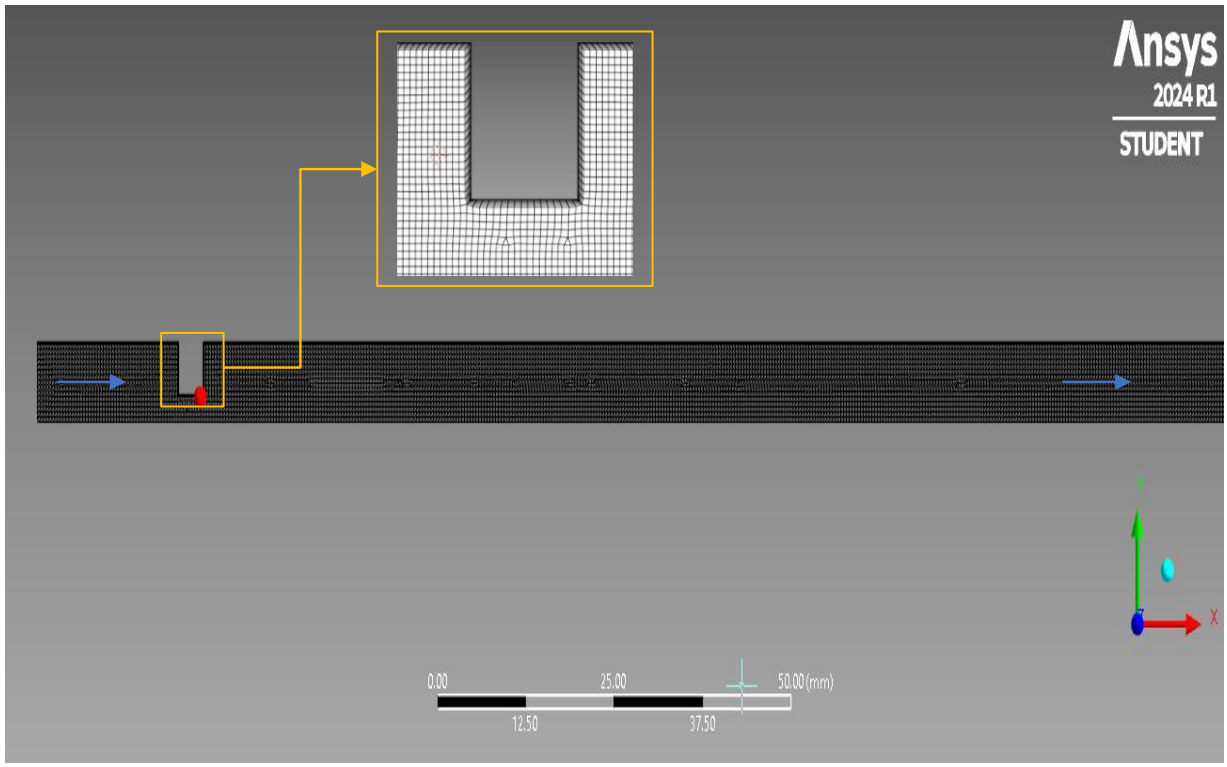


*Figure 4 : Mesh of the geometry*

Table 2, presents the mesh parameters according to β ratio. Due to computational limitations, we performed fine meshing near the orifice plate, and we also performed fine meshing near the wall to capture variations. The necessary boundary conditions were applied at the inlet, outlet, and wall (inlet velocity inlet, wall-to-wall/ no-slip condition, axis-axis, outlet-pressure outlet). The problem was considered to be axis-symmetric.

| β Ratio (mm) | Nodes | Elements |
|---|---|---|
| 4.325 | 109234 | 35723 |
| 5.525 | 109413 | 35780 |
| 6.725 | 109433 | 35784 |
| 7.925 | 109440 | 35793 |

*Table 3: Meshing nodes & elements*

## 2.7 Validation of the present work

At this stage of work, it is necessary to compare the present numerical investigation with the existing and established experimental and numerical work presented by the other researchers to ensure that the present numerical model gives acceptable output in the results.

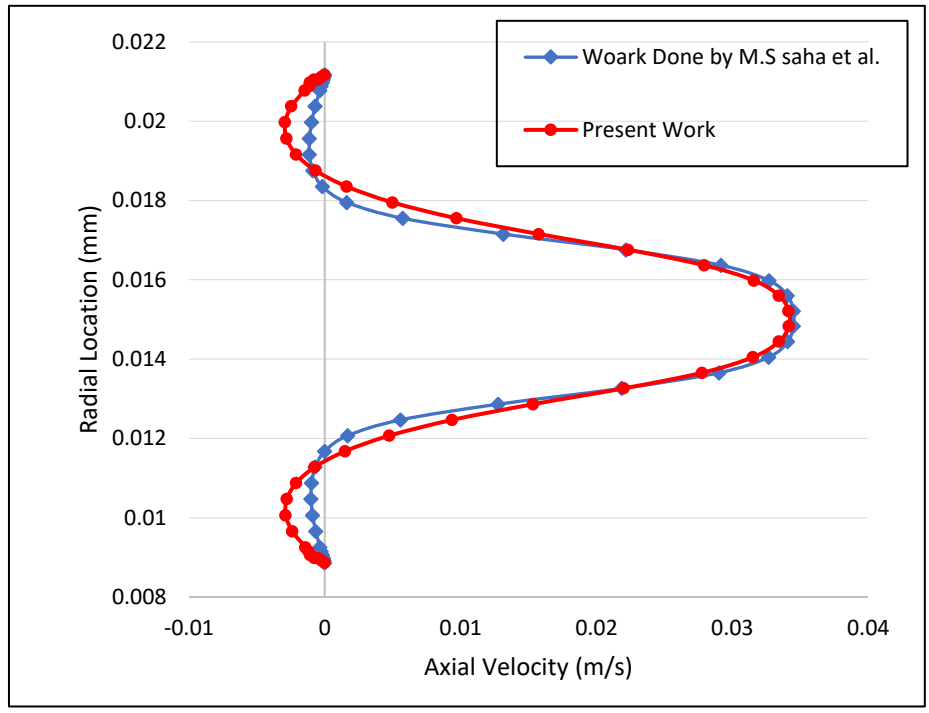


*Figure 5 Validate: Radial velocity profile of the present work and the work presented by M.S Saha et al*

In this work, a comparison between the existing results presented by M.S Saha et al (2012) and the outcome of the present numerical study has been depicted in figure 5 and presented in the subsection of mathematical modeling. In this subsection, the present numerical work has been compared with the work presented by M.S Saha et al (2012) in terms of axial velocity for a specific Reynolds of $10^3$, for a fixed orifice diameter of 12.30 mm and for a fixed length of 494 mm.

From figure 11 it has been seen that the distribution of the axial velocity profile in the present numerical work shows excellent agreement with the numerical investigation presented by the above-mentioned researchers, both in terms of quality and quantity

# CHAPTER 3

## RESULTS AND DISCUSSION OF PRESENT WORK

In this section, the results obtained from the numerical simulations of a square-edge orifice plate through a straight pipe are presented. The parameters chosen for this study are as follows:

1. Streamline contour
2. Velocity contour
3. Pressure contour
4. Turbulence dissipation rate
5. Turbulence kinetic energy

### 3.1. Study of streamline contour

Streamlines are a family of curves whose tangent vectors establish the velocity vector field of the flow thus it shows the flow pattern in the considered domain. Therefore streamline contour has immense role in numerical investigation. In the case of experimental investigation, it is almost impossible to see the flow pattern, as even a high-resolution camera is not able to capture the same. Hence numerical analysis is more advantageous than that of the experimental investigation in terms of obtaining streamline contour.

#### 3.1.1 Effect of Reynolds number on Streamline contours

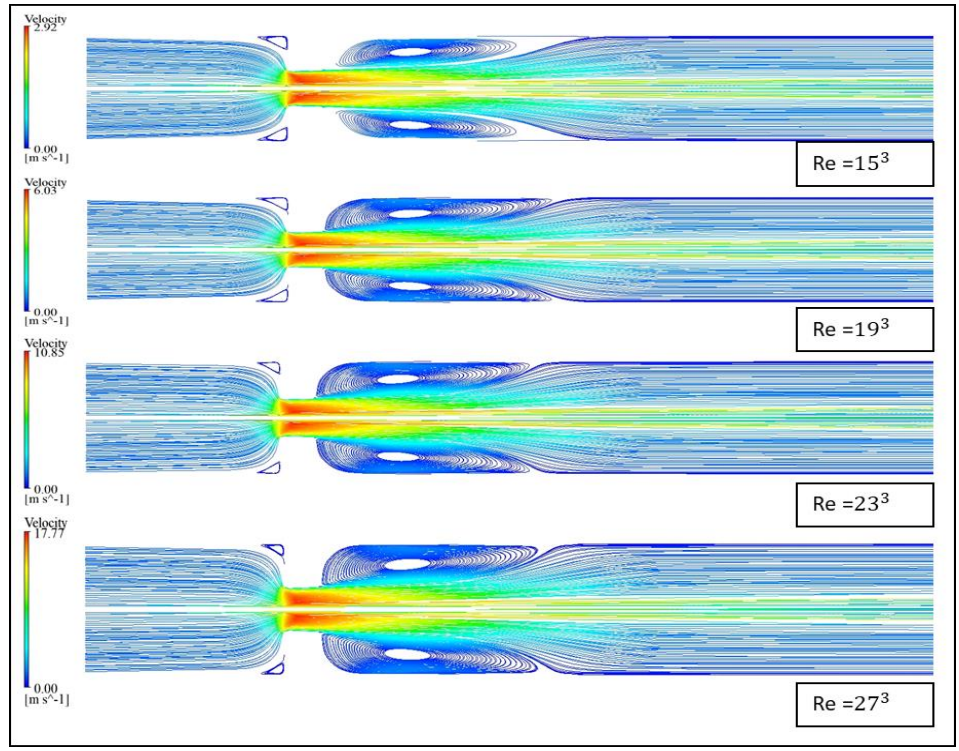


*Figure 6 : Streamline contour for different Reynolds no's.*

Streamline contour for different Reynolds numbers ranging $15^3$ to $27^3$ , for a fixed orifice diameter of 4.325 mm and for a specific thickness of 3.45 mm have been depicted in figure 6. From the figure it has been noted that recirculation bubbles are formed in either side corner of the orifice, Moreover, it has also been seen that the length of the corner recirculating babbles in the downstream Side increases with increasing Reynolds number.

With an increased Reynolds number, the inlet velocity of flow in the orifice is increased as a result of which the length of the corner recirculation zone is enhanced. This may be the possible reason behind the observation. Due to the formation of large size of bubbles, the energy is being lost. Therefore, a lower Reynolds number is involved to minimise the loss of energy.

### 3.1.2 Effect of β ratio on streamlines contour

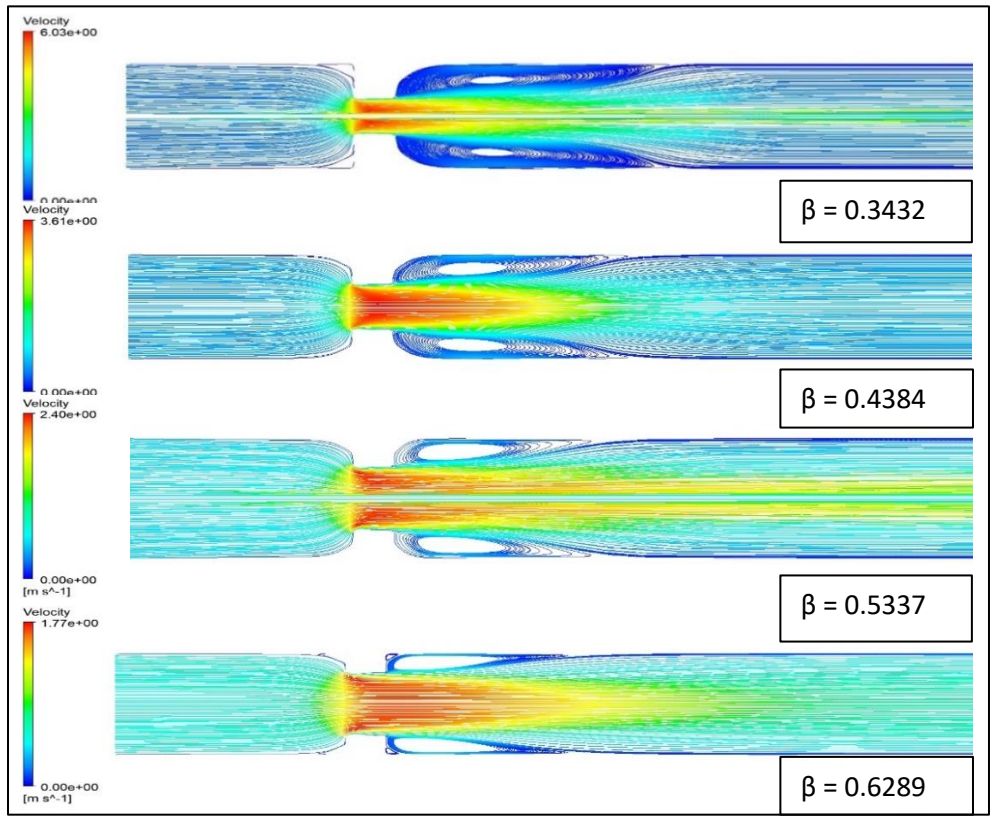


*Figure 7: Streamline contour for different β ratios.*

Streamline contour for different beta ratios (β) ranging from 0.3432 to 0.6289 and the Reynolds number $19^3$ and a specific thickness of 3.45 mm has been depicted in figure 7. From the first contour, it is observed the recirculation bubbles are created in the corner of the orifice upstream side and the length of recirculating bubbles on the downstream side increases, after that, the recirculation bubbles length decreases with increasing the β=0.4384 to 0.6289 ratios, also noted that the vortical structures in the downstream of the flow are drastically weakened.

With an increasing β ratio the recirculation zone is decreased in concert with the length of the orifice. This may be the possible reason behind the observation due to the drastic change in the size of the recirculation structure, due to the low pressure drop. Therefore, the β ratio is involved in minimizing the recirculation zone.

## 3.2. Velocity contour

Velocity contours play an immense role in the numerical investigation. It shows a detailed picture of the flow field, highlighting areas of high and low velocity, and revealing recirculation flow patterns such as vortices, jets, and separation zones. The detailed visualization of the flow patterns of the considered domain provides insights that are not easily accessible through experimental methods.

### 3.2.1 Effect of Reynolds number on velocity contour

Figure 8. shows the velocity contours of a square edge orifice plate, with a diameter of 4.325 mm and a thickness is 3.45 mm for the different Reynolds numbers ranging ( $15^3$ to $27^3$ ) effects of the flow field.

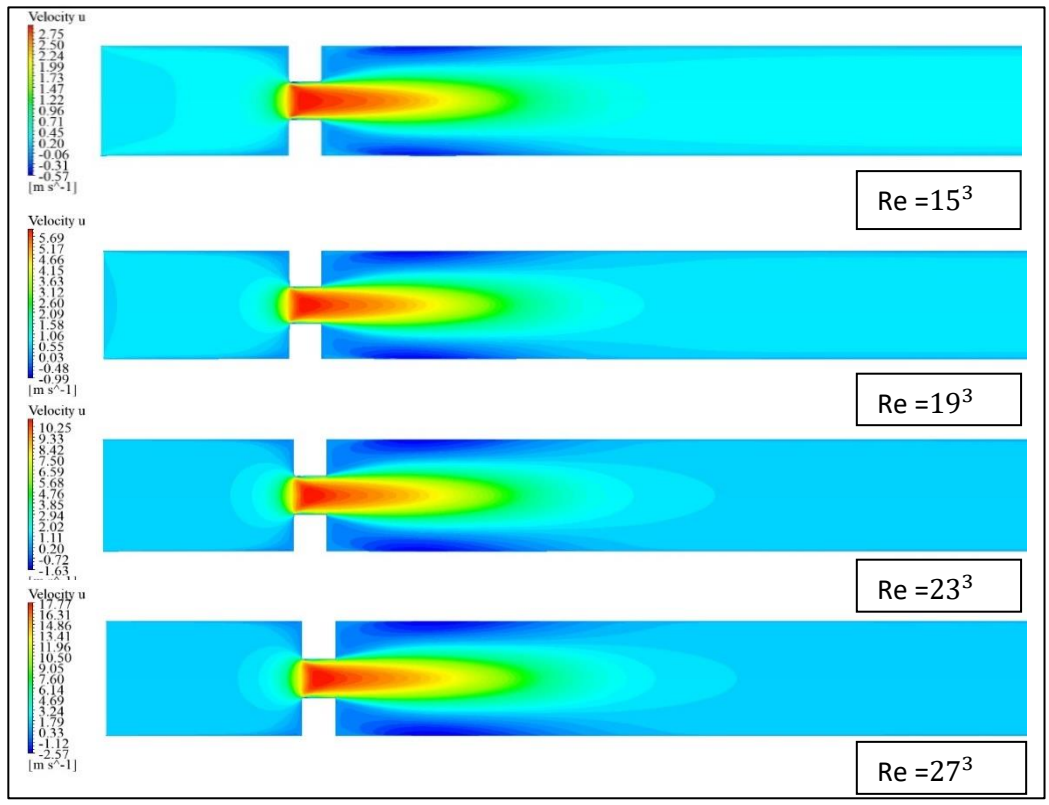


*Figure 8: Velocity Contours Based for different Reynolds no'*

From the figures, it is noted that significantly the orifice influences the flow field, it is observed that the length of the jet is increasing after the orifice, with increasing Reynolds numbers. From the figures, it has been also seen that the direction of velocity changes from negative velocity to positive velocity and vice versa in the corner zone after the orifice. That authenticates the

formation of bubbles at that zone, which have been depicted in the streamline contour. The vortical structure is noted after the orifice near the wall. The separation of the boundary layer, and turbulent wake region was also observed at the downstream side of the orifice plate. Moreover, it has also been seen that the strong velocity gradient near the well upstream and the thin layer disappears with an increased Reynolds number.

### 3.2.2 Effect of β ratio on velocity contour

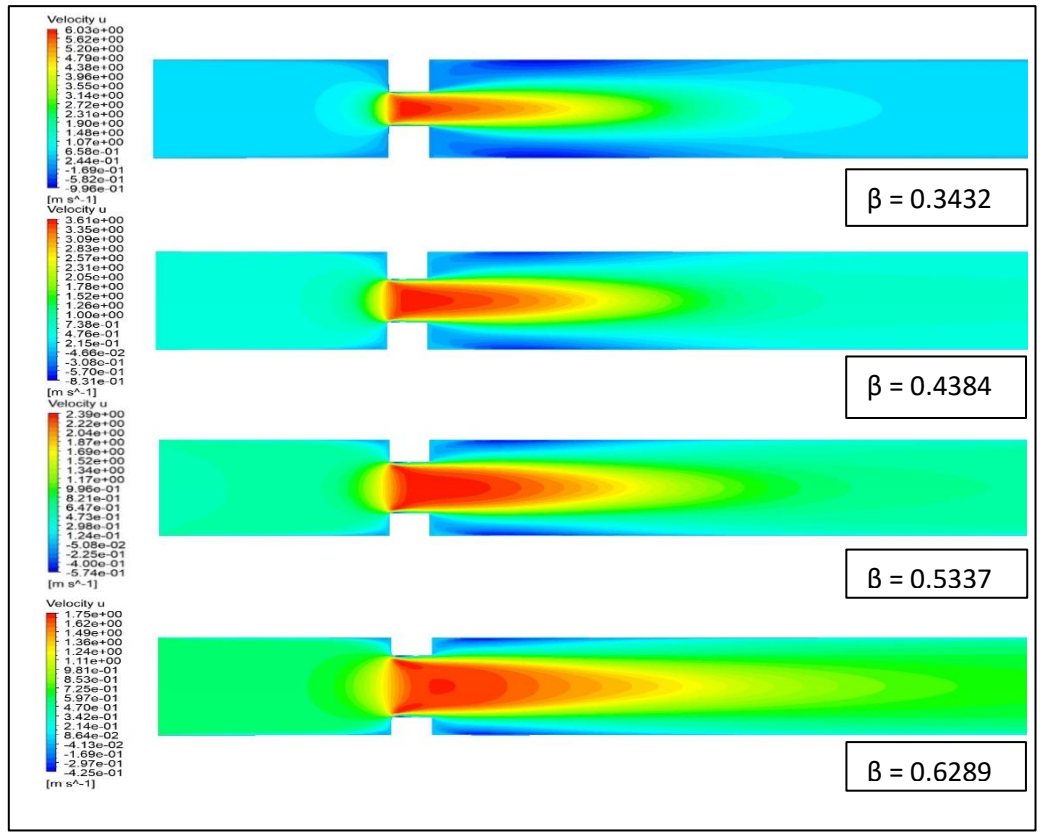


*Figure 9 Velocity Contours Based for different β ratios.*

Figure 9, The velocity contours of a square edge orifice plate, for different beta ratios (β) ranging 0.3432 to 0.6289 and the Reynolds number $19^3$ with a specific thickness of 3.45 mm depicted. It is observed that the acceleration region of the flow passing through the orifice expands with increasing the β ratio, and the jet length also increases. The vortical structures at the corner of the orifice are drastically weakened and slightly reduced with an increase in the β ratio. The Vena contract slightly sifted with an increasing beta ratio.

The pressure drop across the orifice is relatively low since the flow restation is minimal, this may be the possible reason behind the observation due to the drastic change in the size or length of the jet and fluid flow. Moreover, the vortical structure stronger inside the orifice is observed and a small vortical region is formed in the corner of the orifice plate in upstream and the velocity profile is more uniform across the pipe. Therefore, the β ratio is involved in managing the position, strength of the jet, and vena contracta.

## 3.3 Pressure contours

In the numerical investigation, it becomes very challenging to visualize pressure distribution, as even with advanced equipment, it is difficult to obtain a comprehensive view of the pressure field across an entire domain is difficult. The pressure contour provides a clearer visualization, i.e. how the pressure is distributed in different regions of the fluid field. By studying the pressure contours, the critical areas, such as high-pressure zones, low-pressure zones, and pressure gradients, which help to understand the force's behavior, have been identified and the design may be done accordingly

### 4.3.1 Effect of Reynolds number on pressure contour

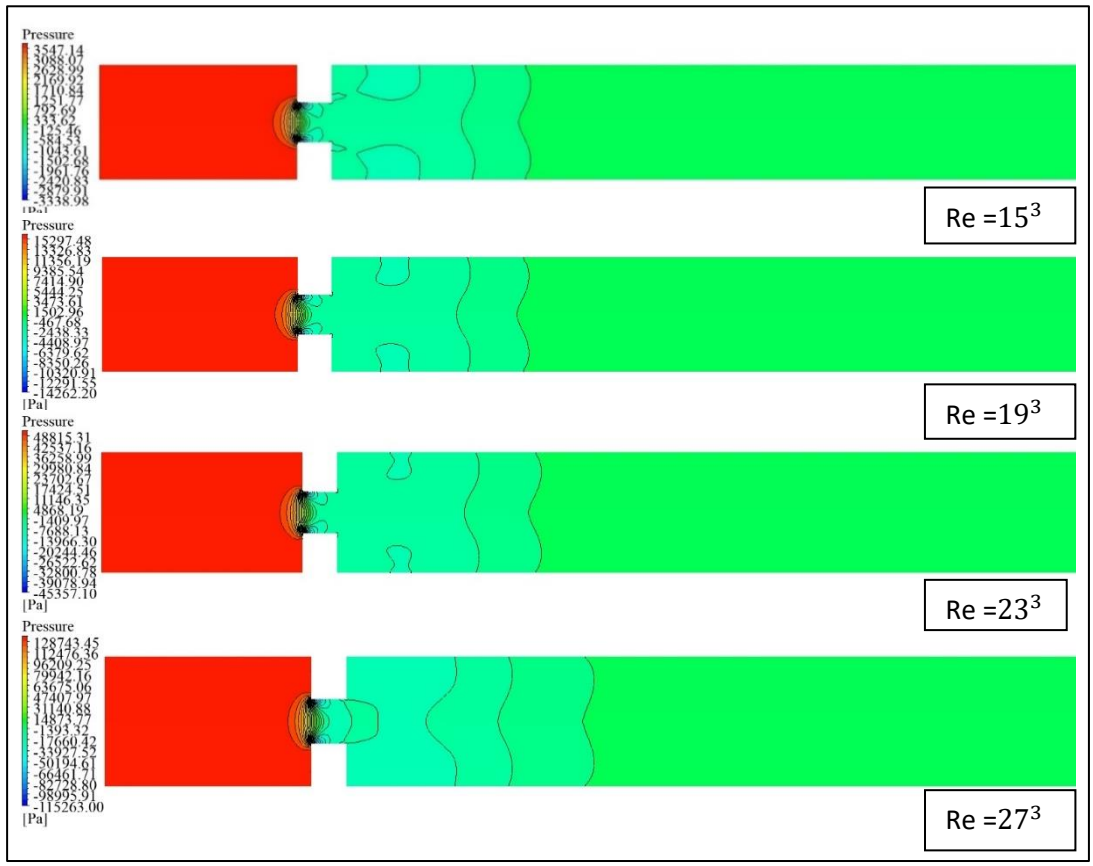


*Figure 10 Pressure Contours Based for different Reynolds no'*

Figure 8, shows the distribution of pressure for various Reynolds number ranges ( $15^3$ to $27^3$ ). From these figures, it is observed that the low-pressure zone was created downstream. The size of the low-pressure zone noted in the downstream well, it is decreased as the Reynolds number increases.

With an increased Reynolds number, the inlet velocity of flow in the orifice is increased because the pressure is dropped, and this may be the possible reason behind the observation, and it satisfies Bernoulli's equation as well. This investigation also validates the present work. Due to the

formation of a low-pressure zone, the energy is lost. Moreover, it has also been observed that a pressure zone is created inside the orifice, and this low-pressure zone increases with increasing the Reynolds number. Therefore, a lower Reynolds number is involved to minimise the loss of energy.

### 3.3.2 Effect of β ratio on pressure contour

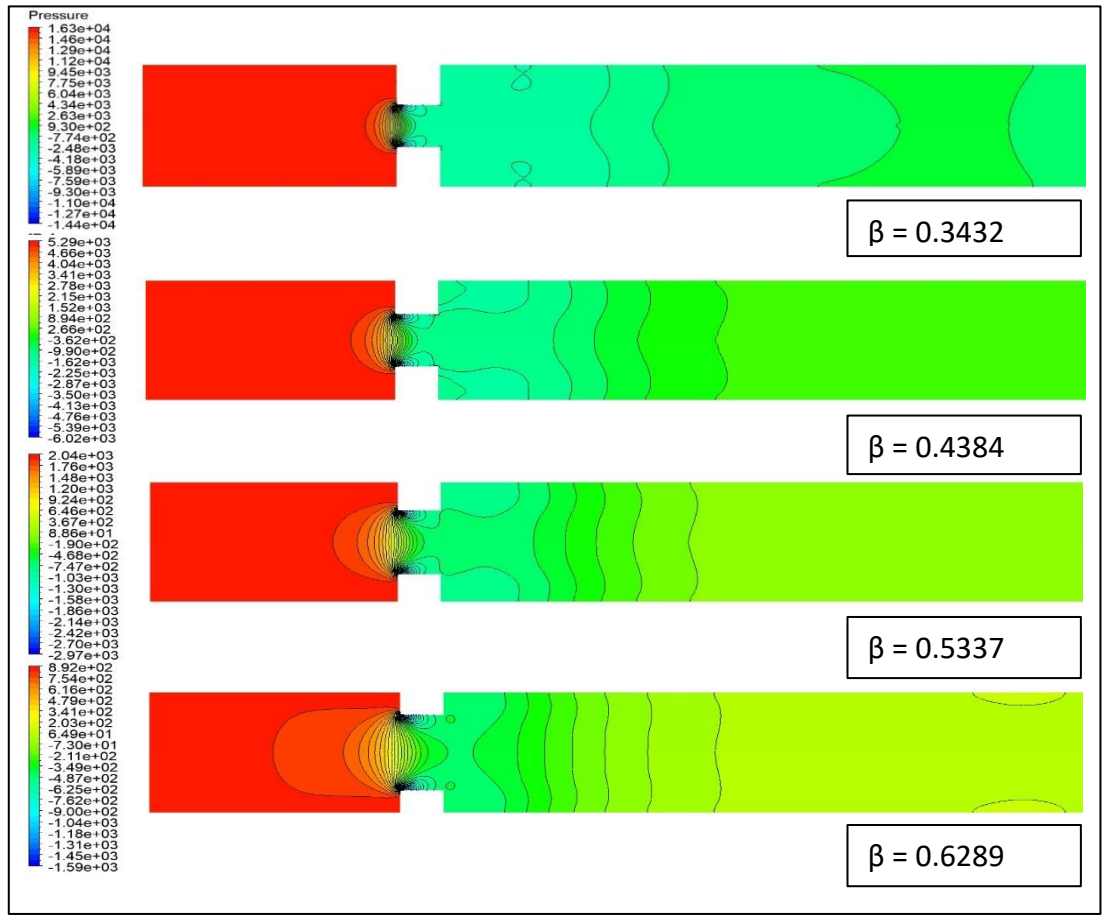


*Figure 11 Pressure Contours Based for different β ratios.*

Figure 9, shows the distribution of pressure for various β ratios. In this figure, we observe the pressure loss decreases with increasing the β ratio.it is visible that the low β ratio profile and low-pressure zone are noted but with an increase in the ratio of β, it is noted that the low-pressure zone is increased.

In the downstream zone, we see a slight reduction in the beta ratio; in the upstream zone, we see some backfired streams due to an increase in the pressure. As the higher beta ratio, pressure drop across the orifice is relatively low since the flow restation is minimal. This may be the possible reason behind the observation due to the drastic change in the size of pressure zones. Therefore, the β ratio is involved in minimizing the pressure drop.

## 3.4 Graphical representation of result discussion

### 3.4.1 Variation of axial velocity and axial pressure for different Re and Beta ratio

Figures 12, show the variation of axial velocity along the length of the pipe. From the figure, it has been noted that the magnitude of axial velocity almost remains the same from the entrance of the pipe to the entrance of the orifice. Just after the orifice the magnitude of axial velocity sharply increased and became maximum at the vena contracta. After the vena contracta, the same is decreased gradually up to an entire length of the pipe, thereafter it again remains unchanged up to the exit of the pipe.

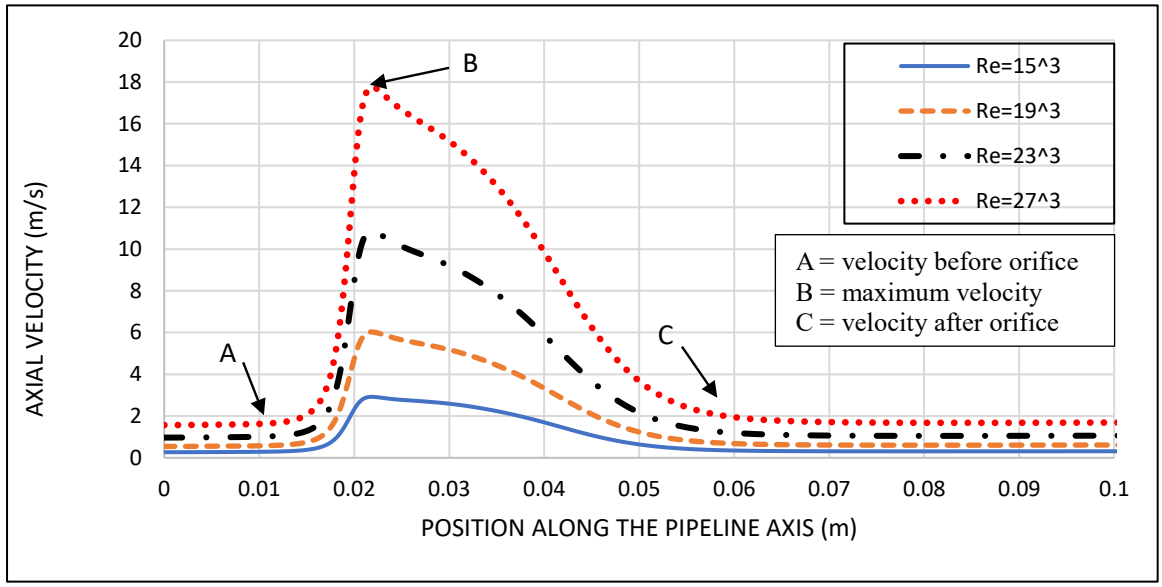


*Figure 12: The variation of axial velocity profiles along the centreline of the test zone.*

| Re | $V_{in}$ (m/s) at point 0.01 | $V_{max}$ (m/s) | $V_{out}$ (m/s) | Position of vena contracta |
|---|---|---|---|---|
| $15^3$ | 0.291 | 2.882 | 0.896 | 0.01 - 0.0228 |
| $19^3$ | 0.578 | 5.964 | 1.297 | 0.01 - 0.0226 |
| $23^3$ | 1.016 | 10.775 | 1.307 | 0.01 - 0.0214 |
| $27^3$ | 1.643 | 17.762 | 1.980 | 0.01 - 0.0218 |

*Table 4 : Velocity of various Reynolds numbers.*

Moreover, it has been also noted that, with increasing Reynolds numbers the magnitude of axial velocity increases. The higher magnitude of the Reynolds number may be the probable reason behind the observation. Therefore, a higher Reynolds number may be recommended in terms of maximum formation fig discharge. Apart from that the position of vena contracta is distomesial, which is a very crucial component to designing an orifice. The position of vena contracta for the considered orifice has been presented as a tabular from Table 4.

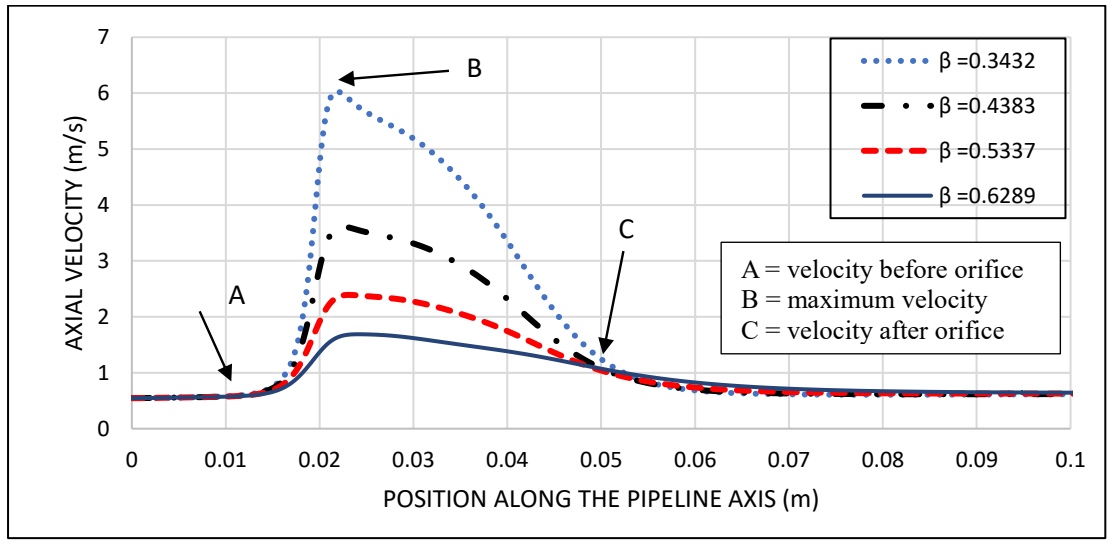


*Figure 13 The variation of axial velocity profiles along the centreline of the test zone.*

| β | $V_{in}$ (m/s) at point 0.01 | $V_{max}$ (m/s) | $V_{out\ at\ point\ 0.0523}$ (m/s) | Position of vena contracta |
|---|---|---|---|---|
| 0.3432 | 0.291 | 6.009 | 1.654 | 0.01 - 0.0222 |
| 0.4383 | 0.578 | 3.612 | 1.501 | 0.01 - 0.0226 |
| 0.5337 | 1.016 | 2.389 | 1.493 | 0.01 - 0.0228 |
| 0.6289 | 1.643 | 1.679 | 1.135 | 0.01 - 0.0230 |

Table 5 The velocity of various Beta ratios

From figure 13, it is considered for different beta ratios, with a fixed Reynolds number $19^3$ and a specific thickness of 3.45 mm for this observation. The center line velocity variations for the orifice with different beta ratios (β = 0.34325, 0.43849, 0.53373, and 0.62897) indicate the maximum velocity occurs for the case of the smallest beta ratio (β = 0.3432) which creates a higher peak velocity and more turbulence, while the low velocity occurs for the largest beta ratio (β = 0.6289), which result in lower peak velocities with less turbulence. The peak point is 0.024 m distance where is the location of the vena contracta. Energy must be conserved at the points in the domain; accordingly, the pressure decreases when the flow approaches the orifice meter, reaching a minimum at vena-contracta, and starts recovering as the flow moves further downstream. Excellent agreement can be seen between the predicted axial velocity profiles.

These observations are due to the value of different inlet velocities and the diagonal restriction. From Figure 12, it has been seen that for all considered Reynolds numbers, the magnitude of axial velocity initially increases a bit near the centreline and then decreases. Figure 13 shows that the beta ratio is the region of the changes in the velocity and the pressure drop of the downstream pipeline. The maximum velocity point for all orifice solutions studied was at the same point of

minimum pressure. When the fluid passes through the orifice, the pressure builds up slightly upstream of the pipe and the fluid is forced to pass through the hole. According to the principle of conservation of energy, at the same time as the velocity increases, the pressure decreases and reaches a minimum value at the point of maximum velocity. The pressure then begins to rise, but no longer reaches the initial value. The results difference between the inlet pressure and that which occurs at a certain distance behind the orifice is related to energy losses, which are caused by the formation of vortices behind the orifice. In figure number 14 and 15, it is observed how the Reynolds number and the beta ratio influence the pressure drop.

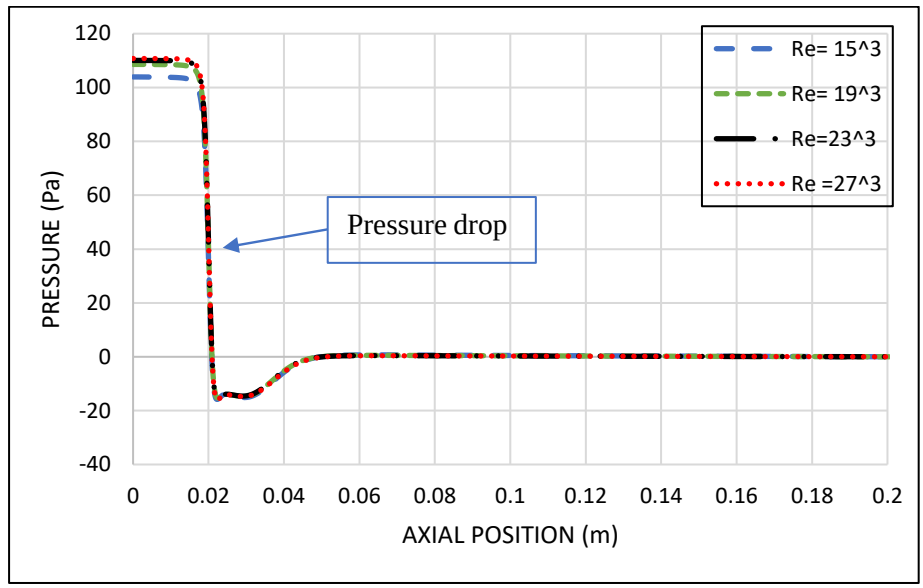


*Figure 14 Axial pressure drops for different Re numbers along the centreline.*

The pressure drops for different Reynolds numbers for 0.0126 m diameter pipe and orifice diameter ratio 0.004325 m and thickness 0.00345 m are shown in figure 14. In this figure, it has been seen that the Reynolds number is inversely proportional to the pressure, where the Reynolds number increases the pressure orifice plate decreases. From figure 14, it has been noted that a pressure drop occurs from point 0.014 m to 0.022 m with reference to the axial position. After this point, a gradual increase in pressure was noted till an axial position of 0.051 m and it remained constant till the end of the pipe. This may be because as the thickness and beta ratio of the orifice, the recirculation length increases, and due to the formation of more vortices, the axial pressure drops at the orifice section increases.

Figure 15, shows the pressure profile for single-phase water flow through orifices of different diameters for Reynolds number $19^3$. clearly shows that the pressure drop, $\Delta P$ across the orifice increases with a decrease in orifice hole diameter and the pressure drop decreases with an increase in beta ratio. When fluid flows from a smaller diameter to a larger one, the recirculation zone height increases. However, a low beta ratio (0.3432) results in a maximum pressure drop from

0.014 m to 0.0224 m. After that, the recovery pressure distance is 0.0454 m in the axial position but the high beta ratio has a low-pressure drop from 0.017 m to 0.023m and its recovery pressure downstream is faster at 0.342 m distance of axial position. Further downstream of the location of minimum pressure (vena contracta), before the recovery pressure point, the pressure till it attains a peak value beyond which the pressure continues to decrease having a negative pressure gradient towards the exit section where the flow re-attains its fully-developed velocity profile possessing a linear negative pressure gradient. The beta ratio and energy conversion rule may be a possible reason for this observation.

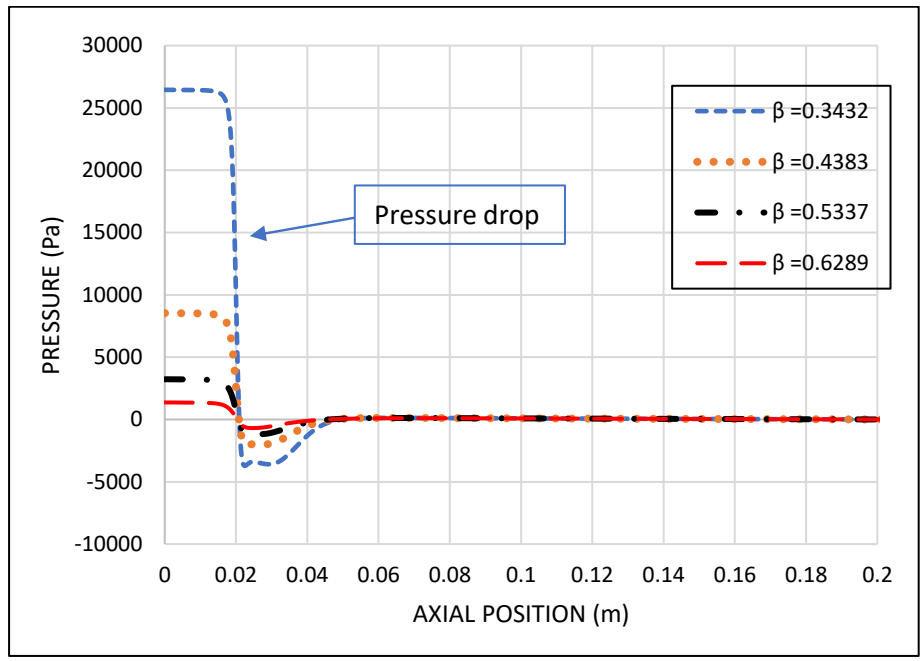


*Figure 15 Axial pressure drops for different beta ratios along the centreline.*

| Reynolds numbers | Pressure Drope ($\Delta P = P1 - P2$) | Beta (β) Ratio | Pressure Drope ($\Delta P = P1 - P2$) |
|---|---|---|---|
| $15^3$ | 102.940 | 0.3432 | 26.276.51 |
| $19^3$ | 107.766 | 0.4383 | 8147.97 |
| $23^3$ | 109.399 | 0.5337 | 3096.25 |
| $27^3$ | 110.109 | 0.6289 | 1241.56 |

*Table 6 pressure drop of various Reynolds number and beta ratios*

## 3.5 Variation of axial velocity effects in different radial locations

The orifice plate restriction has been studied concerning the axial velocity, turbulence kinetic energy, and turbulence dissipation rate at the radial locations at x = 0.024 m, and 0.02745m respectively. This observation warns the readers to check the effect of compressibility on the axial velocity profile in downstream of the orifice plate whenever the Reynolds number is approaching

to its peak value. The plot indicates the reduction of pressure taken with the plot's increased beta value. In the following, the results of the obtained values of axial velocity at two different distances after the orifice are presented. Figures 16 and 17 show the gradual development of fully developed turbulent flow downstream of the orifice plate.

### 3.2.1 Effects of Reynolds numbers

The radial profiles of axial velocity for various Reynolds numbers ranging from $15^3$ to $27^3$ at a fixed axial position of x = 0.024 m and 0.02745m are depicted in Figures 'A' and 'B' respectively. From Figure 16, it has been noted that in all the cases similar kinds of fully developed velocity profiles are formed after the orifice for all considered Reynolds numbers and axial positions. It has also been seen that with increasing Reynolds number, the covering distance to create a fully developed velocity profile is also increasing. Moreover, it has also been observed that with increasing axial location from the orifice, the distance of formation of the fully developed velocity profile is decreased. The axial velocity is more near the orifice, as a result of which, to form a fully developed velocity profile, it covers long distances. Apart from that, due to the increasing Reynolds number, the velocity of flow is also increased consequently, the distance of formation of a fully developed velocity profile is increased. Thus, increasing axial distance and Re may be the probable reason for the above-mentioned observation. Hence, the outcome, which is presented in the figures also validates the present work.

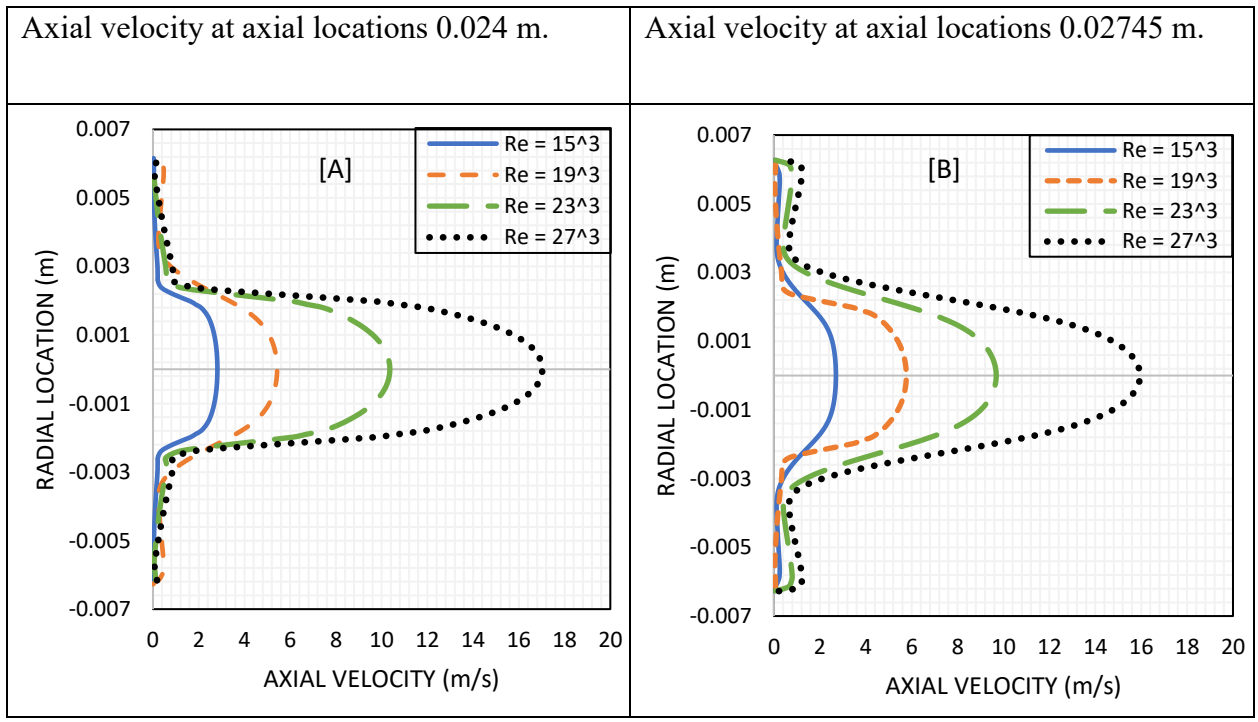


*Figure 16 Radial profiles of axial velocity at axial locations 0.024 m and 0.02745m for different Re.*

### 3.2.1 Effects of Beta Ratios

The radial profiles of axial velocity for various beta ratios ranging from 0.3432 to 0.6289 at a fixed axial position of 0.024 and 0.02745 are depicted in Figures 'C' and 'D' respectively. From the figure 17, it has been noted that, in all the cases similar kinds of fully developed velocity profiles are formed after the orifice for all considered beta ratio and axial positions. It has also been seen that with an increasing beta ratio, the covering distance to create a fully developed velocity profile is also decreased. Moreover, it has also been observed that with increasing axial location from the orifice, the distance of formation of the fully developed velocity profile is decreased. Due to the increasing Beta ratio, the velocity of flow is also decreased consequently, the distance of formation of a fully developed velocity profile is also decreased. Thus, increasing axial distance and beta ratio may be the probable reason for the above-mentioned observation.

| Axial velocity at axial locations 0.024 m for β ratios. | Axial velocity at axial locations 0.02745 m for β ratios. |
|---|---|

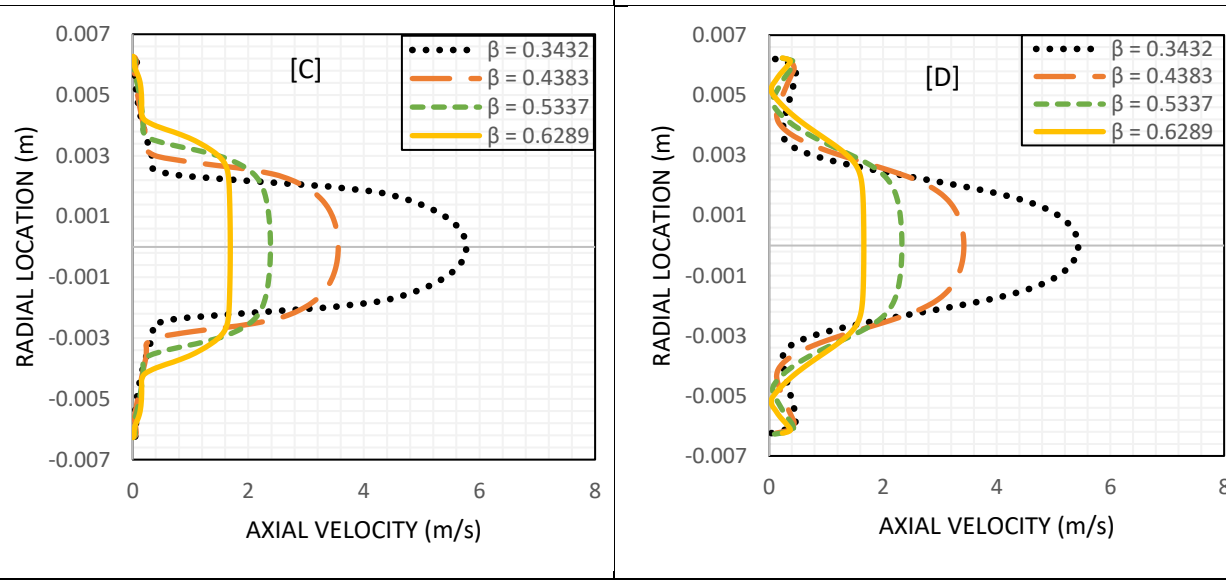


*Figure 17 Radial profiles of axial velocity at axial locations 0.024 m and 0.02745m for different beta ratios.*

| Re | Axial velocity effects in different radial locations | | β | Axial velocity effects in different radial locations | |
|---|---|---|---|---|---|
| | Locations 0.24 m. | Locations 0.2745 m. | | Locations 0.24 m. | Locations 0.2745 m. |
| $15^3$ | 2.81658 | 2.69946 | 0.3432 | 5.77125 | 5.43452 |
| $19^3$ | 5.42843 | 5.7679 | 0.4383 | 3.55598 | 3.42376 |
| $23^3$ | 10.3576 | 9.68402 | 0.5337 | 2.3834 | 2.33412 |
| $27^3$ | 17.0259 | 15.9503 | 0.6289 | 1.68809 | 1.66446 |

*Table 7 Radial profiles of axial velocity at axial locations 0.024 m and 0.02745m.*

## 3.6 Variation of turbulence energy effects in different radial locations

The study analyzes how modifying k-Ɛ turbulence model parameters affects the radial profiles of turbulent kinetic energy (k) and turbulent dissipation rate (Ɛ) downstream of an orifice at various parameters (Reynolds numbers and beta ratio) and distances (0.24m and 0.2457m). Simulations test the sensitivity of these parameters, using a 5% starting turbulence intensity, to establish k and ε. Turbulence's kinetic energy is generated by shear forces and motion agitation, to follow it from the opening to the fully formed turbulent flow. Turbulent kinetic energy is the average kinetic energy per unit mass of fluid in turbulent structures. The dissipation rate (Ɛ) reflects how rapidly this energy is converted to turbulence energy owing to radial velocity.

### 3.3.1 Effects of Reynolds numbers

In Figure 18, profiles (A and B) show the radial distribution of turbulent kinetic energy (k), and profiles (C and D) show the turbulent dissipation rate (Ɛ) at axial distances of 0.24 m and 0.2745 m from the orifice and Table 8 shows effects of variation Reynolds numbers on energy balance. In the profiles of ‘k and Ɛ’ it's observed that, with increasing Reynolds number, the covering distance to create a fully developed turbulent flow profile is also increased. From Figure 19, it has been noted that all the similar kinds of fully developed turbulent profiles formed after the orifice for all considered Reynolds numbers and axial positions. Moreover, it has also been observed that with increasing axial location from the orifice, the distance of formation of the fully developed turbulent kinetic energy and dissipation rate profile is decreased, for the Reynolds number $19^3$, it has been seen that the turbulent kinetic energy and dissipation rate also increase with increase the axial position it is shown in table 8. Due to the increasing Reynolds number, the inertial forces become much larger compared to the viscous forces. Higher inertial forces lead to greater instability in the flow, promoting the formation of turbulence. Thus, Eddies of various sizes superimpose onto the mean flow, increasing axial distance and Re may be the probable reason for the above-mentioned observation.

| Turbulent kinetic energy (k) at axial locations 0.24 m. | Turbulent kinetic energy (k) at axial locations 0.2745 m. |
|---|---|
| 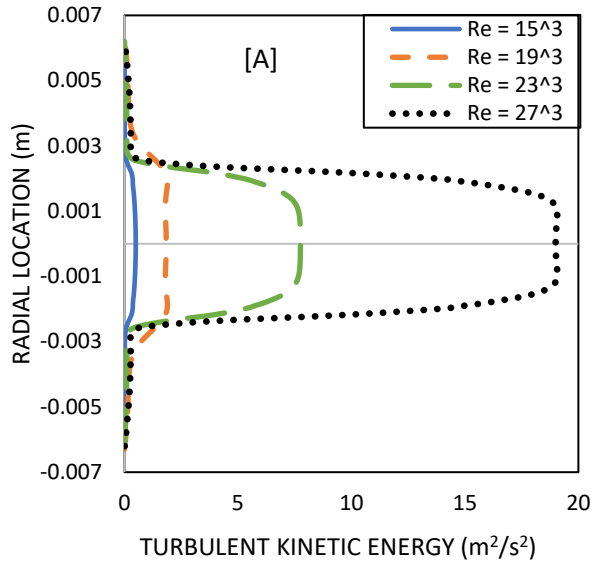 | 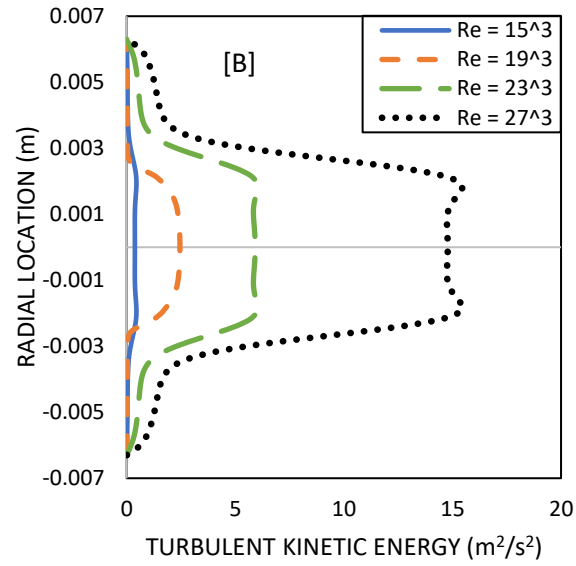 |
| Turbulent dissipation rate (Ɛ) at axial locations 0.24 m. | Turbulent dissipation rate (Ɛ) at axial locations 0.2745 m. |
| 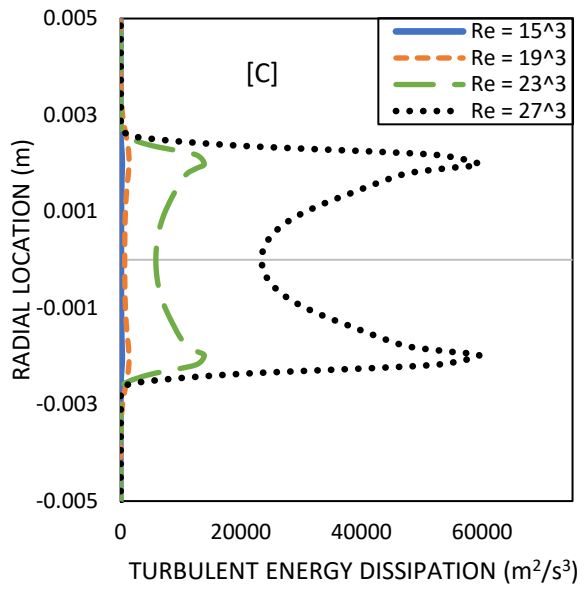 | 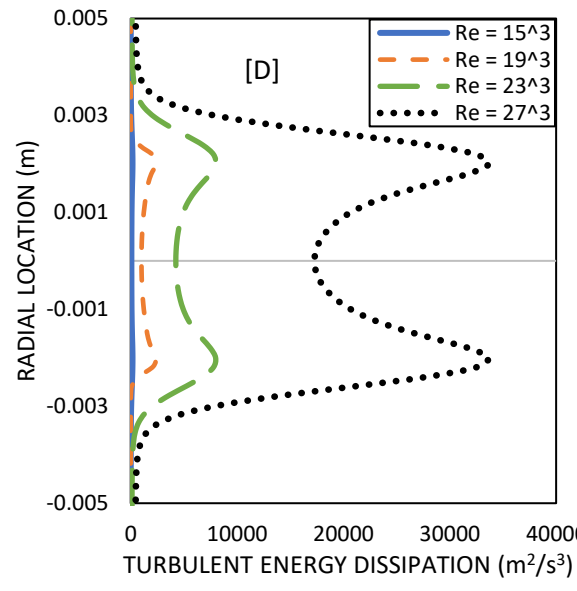 |



*Figure 18 Radial profiles of turbulent kinetic energy (k) and turbulent dissipation rate (Ɛ) at axial locations.*

| Re | Turbulent kinetic energy (k) for axial locations. ($m^2/s^2$) | | Turbulent dissipation rate (Ɛ) for axial locations. ($m^2/s^3$) | |
|---|---|---|---|---|
| | Locations 0.24 m. | Locations 0.2745 m. | Locations 0.24 m. | Locations 0.2745 m. |
| $15^3$ | 0.497571 | 0.377342 | 88.9901 | 65.1083 |
| $19^3$ | 1.84176 | 2.45217 | 721.096 | 1011.88 |
| $23^3$ | 7.75238 | 5.91891 | 5885.06 | 4243.51 |
| $27^3$ | 18.9989 | 14.7828 | 23416.6 | 17275.6 |

Table 8 Radial profiles of turbulent kinetic energy (k) and turbulent dissipation rate (Ɛ) at axial locations.

### 3.3.2 Effects of beta ratio

An orifice creates disturbances in the flow due to the sudden constriction and subsequent expansion of the flow path. These disturbances can cause flow separation and the formation of vortices, leading to turbulence. In the following, the results of the obtained values of turbulent flow at two different distances after the orifice are presented. Figure 19 shows the fully developed turbulent flow downstream of the orifice plate and see a consistent pattern in how turbulence behaves and dissipates in the presence of an orifice, reinforcing the understanding of flow dynamics in such scenarios.

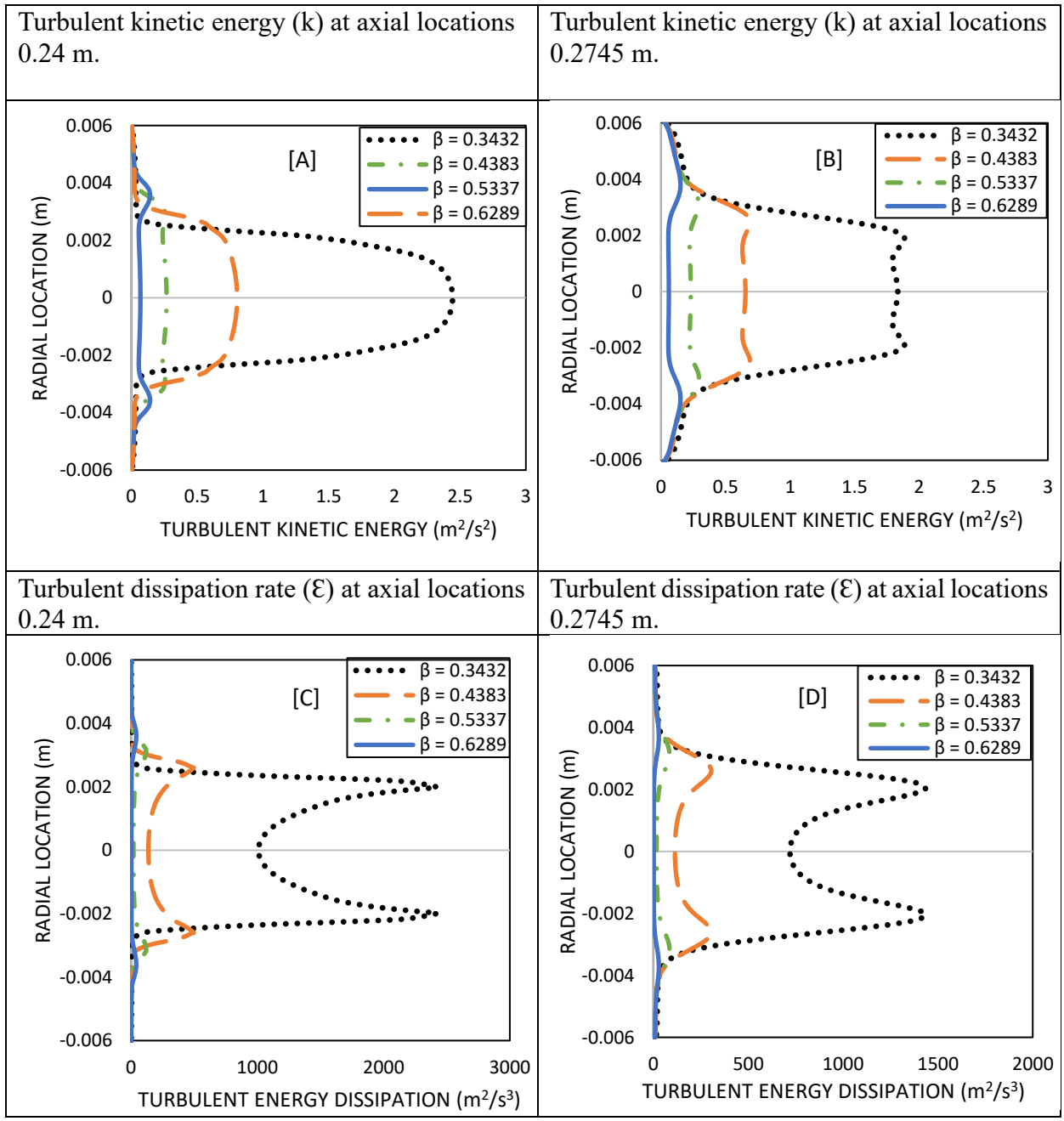


*Figure 19 Radial profiles of turbulent kinetic energy (k) and turbulent dissipation rate (Ɛ) at axial locations*

| β | Turbulent kinetic energy (k) for axial locations. ($m^2/s^2$) | | Turbulent dissipation rate (Ɛ) for axial locations. ($m^2/s^3$) | |
|---|---|---|---|---|
| | Locations 0.24 m. | Locations 0.2745 m. | Locations 0.24 m. | Locations 0.2745 m. |
| 0.3432 | 5.77125 | 5.43452 | 1008.79 | 719.796 |
| 0.4383 | 3.55598 | 3.42376 | 136.739 | 113.387 |
| 0.5337 | 2.3834 | 2.33412 | 18.5173 | 17.0091 |
| 0.6289 | 1.68809 | 1.66446 | 1.857 | 1.75055 |

*Table 9 Radial profiles of turbulent kinetic energy (k) and turbulent dissipation rate (Ɛ) at axial locations.*

The radial profiles of turbulent dissipation rate (Ɛ) at axial distances for various beta ranging from 0.3432 to 0.6289 at a fixed axial position of x = 0.024 m and 0.02745m are depicted in Figures 'A' and 'B' respectively. From figure 19, it has been noted that, in all the cases similar kinds of fully developed turbulent profiles are formed after the orifice for all considered beta ratio and axial positions. It has also been seen that with an increasing beta ratio, the covering distance to create a fully developed Turbulent kinetic energy (k) profiles (A and B) and Turbulent dissipation rate (Ɛ) (C and D) is decreased. Moreover, it has also been observed that with increasing axial location from the orifice, the distance of formation of the fully developed turbulent profile is decreased. The axial velocity is more near the orifice, because of which to form a fully developed turbulent profile it covers long distances. Table 9, clearly noted that Higher beta ratios lead to lower turbulent kinetic energy and dissipation rates and Lower beta ratios result in higher turbulence intensity and dissipation. Thus, increasing beta ratio and lower velocity may be the probable reason for the above-mentioned observation.

# CHAPTER 4

## CONCLUSION

Computational Fluid Dynamics (CFD) simulations have been employed to predict the flow through orifice meters with better accuracy. Specifically, Ansys Student version 2024 solver was used for this purpose. The CFD simulations successfully captured various flow features, including velocity profiles, pressure distribution, and sensitivity analysis of turbulence model parameters. Despite being simple and cost-effective, orifice meters do introduce form friction and lead to some unrecovered pressure drop. At present numerical studies are considered in two different flow regimes, Beta ratio at $0.3432 \leq \beta \leq 0.6289$ and Reynolds number at $15^3 \leq Re \leq 27^3$. The numerical simulations are based on Navier-Stokes equations under the assumption that the flow is incompressible and viscous, and a $k - \varepsilon$ turbulence model has been used for the turbulent flow regime. The main conclusions are as follows:

1. The jet flow out of the orifice increases slightly with increasing $Re$. The acceleration region of the flow passing the orifice expands with increasing β, and the length of the jet flow expands.
2. The recirculation length of the flow increased with an increasing Reynolds number, and the inlet velocity of flow in the orifice is also increased as a result of which the length of the corner recirculation zone is enhanced and the recirculation bubbles length decreases with increasing the β ratios, also found the vortical structures in the downstream of the flow are drastically weakened.
3. The orifice influences the flow field, it is observed that the length of the jet is increasing after the orifice, with increasing Reynolds numbers. The direction of velocity changes from negative to positive in the corner zone after the orifice, and vice versa. The size of the vortical structure becomes smaller in the cross-section direction while becoming larger in the streamwise direction with an increase in Reynolds numbers. At higher Reynolds numbers, the vortical region around the shear layer behind the orifice plates becomes weaker, and small irregular vortices appear around the corner of the orifice plate. The vortical structures at the corner of the orifice are drastically weakened and slightly reduced with an increase in the β ratio. The vena contract slightly sifted with an increasing beta ratio.

4. The proposed design of an orifice meter includes a provision to track vena contracta using CFD techniques. It has been explained and demonstrates a predicted linear relationship between the flow rate and the maximum pressure drop through an orifice (ΔP). With rising Reynolds numbers the pressure drop is increased but the increasing the beta ratio the pressure drop is decreased. However, its performance must be evaluated numerically in small-sized pipelines before the design can be applied to larger bore pipelines.
5. The study investigates the impact of modifying k-Ɛ turbulence model parameters on the radial profiles of turbulent kinetic energy (k) and turbulent dissipation rate (Ɛ) downstream of an orifice at various Reynolds numbers and beta ratios, and distances (0.24m and 0.2457m). The findings indicate that with increasing Reynolds numbers, the distance required to establish a fully developed turbulent flow profile also increases. Additionally, as the axial location from the orifice increases, the formation distance for a fully developed turbulent kinetic energy and dissipation rate profile decreases. For a Reynolds number of $19^3$, it is observed that both the turbulent kinetic energy and dissipation rate increase with the axial position. Moreover, higher beta ratios result in lower turbulent kinetic energy and dissipation rates, whereas lower beta ratios lead to higher turbulence intensity and dissipation.

## Future Study:

1. Study the potential structural vibration caused by flow through the orifice with different characteristics and at various Reynolds numbers.
2. Study the multiphase flow through an orifice, examining its behavior and comparing it with single-phase flow.
3. Study the flow through multi-hole orifices, venturi, and nozzle-shaped flow meters. Compare different obstruction shapes and determine suitable areas for the application of the different obstruction flow meters.

## Publication :

Significant research papers on Numerical CFD simulations have been submitted for publication, reflecting advancements in this field.

A paper, "**Numerical analysis on the characteristics of a fluid flowing through an orifice in a marine piping system**," has been submitted to the prestigious journal with the help of my guide. I am presented at the International Conference on Recent Advances in Fluid Mechanics and Nanoelectronics **(ICRAFMN 2024)**. This conference, organized by the Manipal Institute of Technology in Jaipur, provided a platform for discussing the latest advancements and research in the field. My conference id **ICRAFMN_2024-FD-282** .

# REFERENCE


1. Smith Eiamsa-ard, Ariti Ridluan. (2008). Numerical Investigation of turbulent flow through a. *KMTIL Science Journal, 8*(1).
2. D.Chisholm. (1983). Two-phase flow in pipelines and heat Exchangers. *London: Longman Group Education* .
3. M, C. (2006). Flow measurement. *Missouri University of Science and Technology*.
4. Biryuk Vladimir Vasilevich, Eliseev Yurij Sergeevich, Kirsanov Yurij Georgievich, Livshits Mikhail Yurevich, Sheludko Leonid Pavlovich, Shimanov Artem Andreevich. (2006). Method Of Desalination Plant Operation With Multi-Stage Evaporators And Steam Compressor And Installation For Its Implementation. *Russian Federation Service*, 2-5.
5. Anish. (2019, July 5). *General Overview of Central Cooling System on Ships*. Retrieved from Marine in Site: https://www.marineinsight.com/guidelines/general-overview-of-central-cooling-system-on-ships/
6. Dr Michael Pritchard, Advantica Mr David Marshall, Advantica Mr John Wilson. (2004). An Assessment Of The Impact Of Contamination On Orifice Plate Metering Accuracy. *North Sea Flow Measurement Workshop* .
7. Sethi, S. (2021, May 27). *Marine Freshwater Generators: Common Problems And Solutions*. Retrieved from Marine in Site: https://www.marineinsight.com/guidelines/troubleshooting-marine-freshwater-generators/
8. Staff, E. (2023). *Basics of Orifice Plates*. Retrieved from Inst Tools: https://instrumentationtools.com/orifice-plates/
9. *Types of Orifice Plates Used in Flow Measurement*. (n.d.). Retrieved from Instrumentation Toolbox: https://www.instrumentationtoolbox.com/2013/02/introduction-to-orifice-plates.html:google_vignette
10. ABB. (2024). *Differential pressure – primary flow element orifice plates and orifice flange unions.*
11. *Laminar and Turbulent Flow - Characteristics, Difference, and Applications*. (2023, July 29). Retrieved from Testbook: https://testbook.com/civil-engineering/laminar-and-turbulent-flow-definition
12. *Sea Water Flow Measurement*. (2023, July 14). Retrieved from Supmea: https://www.supmeaauto.com/training/sea-water-flow-measurement
13. *Marine Ship Flow Measurement Solutions*. (2022, December 27). Retrieved from Microsensor: https://www.microsensorcorp.com/Details_Marine-Ship-Flow-Measurement-Solutions.html
14. *Concentric, Eccentric & Segmental Orifice Plates*. (n.d.). Retrieved from Control And Instrumentation: https://www.controlandinstrumentation.com/flow/orifice-plate-type.html.
15. Lu He, Francisco Ruiz. (1995). Effect Of Cavitation On Flow And Turbulence In Plain Orifices For High-Speed Atomization. *Atomization and Sprays, 5*(6).
16. N Abed, H F Hassan, Amer Al-damook, W H Khalil. (2020). Experimental and numerical. *Materials Science and Engineering, 881*.
17. A. Erdal and H. I. Andersson. (1997). Numerical aspects of flow computation through orifices. *Flow Measuring Instrument, 8*(1), 27-37.

18. Y. S. Ho and T. P. Leung. (1985). Performance of conical entrance orifice plates at low Reynolds numbers. *International Journal of Heat and Fluid Flow*, 122 -125.

19. Markatos, N. C. (1986). The mathematical modelling of turbulent flows. *Appl. Math. Modelling, 10*, 190-220.

20. G. L. Morrison, K. R. Hallt, J. C. Holste, M. L. Macek, L. M. Ihfe, R. E. Deotte and D. P. Terracina. (1994). Comparison of orifice and slotted plate flowmeters. *Flow Measurement Instrument, 5*(2), 71 - 77.

21. Feng Shan, Zhichun Liu, Wei Liu, Yoshiyuki Tsuji. (2016). Effects of the orifice to pipe diameter ratio on orifice flows. *Chemical Engineering Science, 152*, 497 - 506.

22. Boualem Laribi, Abdelaziz Aït Amrane, and Abdelkader Youcefi. (2013). Numerical analysis of the discharge coefficient with disturbers for flowmetring accuracy. *International Congress of Metrology*.

23. Junxia Gao & Fenghe Wu. (2019). Investigation of flow through the two-stage orifice. *Engineering Applications of Computational Fluid Mechanics,, 13*, 117-127.

24. C.L. Hollingshead, M.C. Johnson, S.L. Barfuss, R.E. Spall. (2011). Discharge coefficient performance of Venturi, standard concentric orifice plate, V-cone and wedge flow meters at low Reynolds numbers. *Journal of Petroleum Science and Engineering, 78*, 559-566.

25. Tian-Ming Ding and Yuanjiao Wang. (2015). Comparison Research on Hydraulic Characteristics of Three Type's Orifice Plate. *The Open Fuels & Energy Science Journal, 8*, 43-46.

26. S. H. Alvi, K. Sridharan ,N. S. Lakshmana rao. (1978). Loss Claracteristics if Orifices ai l lizzies. *Journal of Fluid Engineering, 100*, 299-307.

27. Naveenji Arun. (2010). CFD Analysis On Discharge Co Efficient During Non Newtonian Flows Through Orifice Meter. *International Journal of Engineering Science and Technology, 2*(7), 3151-3164.

28. Mara Nilza Estanislau Reis, Wender Pereira de Oliveira, Pedro Américo Magalhães Junior, . (2019). Incompressible Flow At Low Reynolds Number In A Conical Entrance Orifice Plate. *25th ABCM International Congress of Mechanical Engineering*, 20-25.

29. Hasan Bulut, Mahmut Ergut, Vedat Asil,Roza Horvath Bokor, 2004. Numerical solution of a viscous incompressible flow problem through an orifice by Adomian decomposition method. *Applied Mathematics and Computation,* Volume 153, pp. 733-741.

30. Robert W. Hornbeck. (2015). Laminar Flow In The Entrance Region Of A Pipe. *Applied Science Research, 13*, 224-234.

31. B.Sahin and H. Ceyhan. (1996). Numerical and experimental analysis of laminar flow through square edged orifice with variable thickness. *Trans Inst, 18*(4), 166-174.

32. Marko Đurđević, Maša Bukurov, Slobodan Tašin And Siniša Bikić. (2019). Experimental Research Of Single-Hole And Multi-Hole Orifice Gas Flow Meters. *Flow Measurement and Instrumentation*, 1-15.

33. A P Jurga, M J Janocha, G Yin, K E T Giljarhus and M C Ong. (2021). Validation and assessment of different RANS turbulence models for simulating turbulent flow through an orifice plate. *IOP Conf. Series: Materials Science and Engineering*, 1-16.

34. Zahra Abbas-Shiroodi , Mohammad-Taghi Sadeghi, Soroush Baradaran. (2021). Design and optimization of a cavitating device for Congo red decolorization: Experimental investigation and CFD simulation. *Ultrasonics Sonochemistry*.

35. Ning HE, Zhen-xing ZHAO. (2010). Theoretical and numerical study of hydraulic characteristics of orifice energy dissipator. *Water Science and Engineering, 3*(2), 190-199.

36. Sravani Vemulapalli, Santhosh Krishnan Venkata. (2022). Parametric analysis of orifice plates on measurement of flow: A review. *Ain Shams Engineering Journal*.

37. Suat Canbazog˘lu, Fazıl Canbulut. (2005). A note on the flow coefficients of capillary tube and small orifice restrictors exposed to very low Reynolds number flow. *Industrial Lubrication and Tribology, 57*(3), 116-120.

38. Abdulrazaq A. Araoye, Hasan M. Badr,Wael H. Ahmed. (2017). Investigation of flow through multi-stage restricting orifices. *Annals of Nuclear Energy*, 75-90.

39. C. R. Sanghani,D. C. Jayani,C. R. Dobariya,G. K. Sabhadiya,J. R. Gohil. (2016). Comparative Analysis of Different Orifice Geometries for Pressure Drop. *International Journal of Science Technology & Engineering, 2*(10), 494-498.

40. Prabhata K. Swamee & Nimisha Swamee. (2010). Discharge equation of a circular sharp crested orifice. *Journal of Hydraulic Research*, 106-109.

41. Malatesh Barki,Ganesha T,Dr. M. C. Math. (2014). CFD Analysis and Comparison of Fluid Flow Through A Single Hole And Multi Hole Orifice Plate. *International Journal of Research in Advent Technology, 6*(5), 6-15.

42. Gianpietro Di Rito. (2007). Experiments and CFD Simulations for the Characterisation of the Orifice Flow in a Four-Way Servovalve. *International Journal of Fluid Power*, 37-46.

43. Saeed Ahmed, Aitazaz Hassan, Rehan Zubair, Shahid Rashid,Atta Ullah. (2023). Design modification in an industrial multistage orifice to avoid cavitation using CFD simulation. *Journal of the Taiwan Institute of Chemical Engineer*.

44. Xueping Gao, Han Zhang, Jijun Liu, Bowen Sun & Ye Tian. (2018). Numerical investigation of flow in a vertical pipe inlet/outlet with a horizontal anti-vortex plate: effect of diversion orifices height and divergence angle. *Engineering Applications of Computational Fluid Mechanics, 2*(1), 182-194.

45. Michael Reader-Harris, Neil Barton, David Hodges. (2012). The effect of contaminated orifice plates on the discharge coefficient. *Flow Measurement and Instrumentation,* 2-7

46. Mara N.E. Reis, Sergio Hanriot. (2017). Incompressible Pulsating Flow For Low Reynolds Numbers In Orifice Plates. *Flow Measurement and Instrumentation.*

47. Manmatha K. Roul, Sukanta K. Dash. (2012). Single-Phase and Two-Phase Flow Through Thin and Thick Orifices in Horizontal Pipes. *Journal of Fluids Engineering, 134*.

48. K. Rup, P. Sarna. (2011). Analysis of turbulent flow through a square-sectioned duct with installed 90-degree elbow. *Flow Measurement and Instrumentation, 22*, 383-391.

49. Katharina Schrank, Hubertus Murrenhoff, Christian Stammen. (2013). Cfd Simulations And Experiments Of The Dispersed Two-Phase Flow Through Hydraulic Orifices. *Fluids Engineering Division Summer Meeting.*

50. K H Yau, E C Kua, and S Balvinder. (2017). Numerical investigation of a thick plate restriction orifice on the pressure drop performance. *Materials Science and Engineering*.

51. D Zahariea. (2016). Numerical analysis of eccentric orifice plate using ANSYS Fluent software. *Materials Science and Engineering*.